

**DESIGN AND DEVELOPMENT OF RENEWABLE
ENERGY BASED MICROGRIDS WITH GRID
SYNCHRONIZATION AND THEIR APPLICATIONS
TO EV CHARGING INFRASTRUCTURE**

PAVITRA SHUKL



**DEPARTMENT OF ELECTRICAL ENGINEERING
INDIAN INSTITUTE OF TECHNOLOGY DELHI
JULY 2022**

© Indian Institute of Technology Delhi (IITD), New Delhi, 2022

**DESIGN AND DEVELOPMENT OF RENEWABLE
ENERGY BASED MICROGRIDS WITH GRID
SYNCHRONIZATION AND THEIR APPLICATIONS
TO EV CHARGING INFRASTRUCTURE**

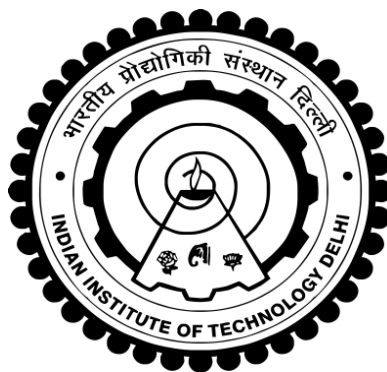
by

PAVITRA SHUKL

Electrical Engineering Department

Submitted

*in fulfillment of the requirements of the degree of **Doctor of Philosophy**
to the*



**INDIAN INSTITUTE OF TECHNOLOGY DELHI
JULY 2022**

CERTIFICATE

It is certified that the thesis entitled “**Design and Development of Renewable Energy Based Microgrids with Grid Synchronization and Their Applications to EV Charging Infrastructure,**” being submitted by **Mrs. Pavitra Shukl** for award of the degree of **Doctor of Philosophy** in the Department of Electrical Engineering, Indian Institute of Technology Delhi, is a record of the student work carried out by her under my supervision and guidance. The matter embodied in this thesis has not been submitted for award of any other degree or diploma.

Dated: 29th July 2022

(Prof. Bhim Singh)
Electrical Engineering Department
Indian Institute of Technology Delhi
Hauz Khas, New Delhi-110016, India

ACKNOWLEDGEMENTS

I wish to express my sincere gratitude and indebtedness to **Prof. Bhim Singh** for providing me guidance and constant supervision to carry out the Ph.D. work. Working under him has been a wonderful experience, which has provided a deep insight to the world of research. Determination, dedication, innovativeness, resourcefulness and discipline of **Prof. Bhim Singh** have been the inspiration for me to complete this work. His consistent encouragement, valuable advice, continuous monitoring and commitments to excellence have always motivated me to improve my work and use the best of my capabilities. It was due to his blessing that I have experienced new traits of technical research and have earned various other experiences, which will help me throughout my life.

I express my deep gratitude and sincere thanks to **Prof. Sukumar Mishra, Prof. G. Bhuvaneswari and Prof. Ashu Verma**, SRC members for their valuable guidance and consistent support during my research work.

I wish to convey my sincere thanks to **Prof. Bhim Singh, Prof. B. P. Singh, Prof. M. L. Kothari and Prof. Anandarup Das** for their valuable inputs during my course work, which made the foundation for my research work. I am grateful to IIT Delhi for providing me the necessary research facilities. Thanks are due to Sh. Srichand, Sh. Puran Singh, Mr. Jitendra and Mr. Anurag of PG Machines Lab, IIT Delhi for providing me facilities and assistance during this work.

I am greatly thankful to Dr. Ikhlaq Hussain, Mr. Anshul Varshney, Dr. Shailendra Kumar, Dr. Shadab Murshid, Dr. Anjaneesh Mishra, Dr. Tabish Mir, Dr. Radha Kushwaha, Dr. Seema, Dr. Utkarsh Sharma, Dr. Nidhi Mishra, Dr. Subarni Pradhan, Dr. Aniket Anand, Dr. Chinmay Jain, Dr. Geeta Pathak, Dr. Rajan Sonkar, Dr. Sachin Devassy, Dr. Nishant Kumar, Dr. Sai Pranith Girimaji, , Dr. Piyush Kant, Dr. Saurabh Shukla, Dr. Deepu Vijay, Dr. Priyank Shah and Dr. V.L. Srinivas for their valuable aid, co-operation and informal support during this period.

I convey my heartfelt and sincere thanks to Ms. Farheen Chisti, Ms. Shubhra and Ms. Rohini for continuous cooperation, motivation and informal support during my research work. I would also like to thank Mr. P. Sambasivaiah and Mr. Munesh Kumar Singh for being supportive. I am thankful to Ms. Vanadana Jain and Ms. Shatakshi Sharma, for their valuable aid and co-operation. Moreover, I would like to thank, Ms. Smita, Mr. Sreejith R, Mr. Gurmeet Singh, Mr. Anjeet Verma, Mr. Debasish Mishra, Mr. Vineet P. Chandran, Mr. K. P. Tomar, Mr. Sunil Kumar Pandey, Ms. Yashi Singh, Ms. Hina Parveen, Ms. Rashmi Rai, Ms. Farha, Mr. Yalavarthi Amarnath, Mr. Arayadip Sen, Mr. Kashif, Mr. Gaurav Modi, Mr. Sudip Bhattacharya, Mr. Bilal Naqvi, Mr. Jitendra Gupta, Mr. Utsav Sharma, Mr. Sandeep Kumar Sahoo, Ms. Shalvi Tyagi, Mr. Souvik Das, Mr. Vivek Narayanan, Mr. Saran Chaurashiya, Mr. Sharan Shastri, Mr. Shivam Yadav, Mr. Rahul Kumar, Mr. Deepak Saw, Ms. Kousalya V, Ms. Chandrakala Devi, Ms. Kripa and all PG Machines lab group for their valuable support.

I would also like to thank Mr. Yatindra, Mr. Satish, Mr. Sandeep and all other Electrical Engineering office staff for being supportive throughout. I am likewise thankful to those who have directly or indirectly helped me to finish my dissertation study.

I would like to thank my mother, Mrs. Purnima Shukla, my father Mr. Pradeep Kumar Shukla, mother-in-law Dr. Jyoti and father-in-law Mr. Krishna Chandra Mishra for their blessings and constant encouragement. Moreover, I would like to thank my husband Mr. Kumar Varun for giving me the inner strength and wholehearted support. I would like to thank my younger brother Shivam Shukla and sister-in-law Ms. Shreya Mishra for their continuous support and encouragement. Their trust in my capabilities had been a key factor to all my achievements. At last, I am beholden to almighty for their blessings to help me to raise my academic level to this stage. I pray for their benediction in my future endeavors. Their blessings may be showered on me for strength, wisdom and determination to achieve in future.

Date: 29th July 2022

Pavitra Shukl

ABSTRACT

This work focuses on the utilization of hybrid distributed energy resources such as solar, wind, battery and fuel cell sources based microgrids with applications to the electric vehicles (EVs) charging infrastructure. The usage of microgrids addresses the problems related to the electrification of remote areas along with the ability to synchronize with the utility grid. Thus, with the utilization of renewable energy sources and energy storage devices, the problems to feed the remote locations along with reduction in fossil-fuels consumption can be resolved. In addition, the EVs connected to the microgrids for charging purposes, act as highly flexible loads, with additional storage capacity and offers the advantages of reduction in harmful emissions, thereby, guaranteeing environmental friendly transportation.

The microgrids consisting of renewable energy sources such as solar PV array, wind turbine and fuel cell stack are utilized here, which work in synchronicity with the utility grid along with power transfer to the local loads and charging of EVs. Moreover, the microgrid reliability is dependent upon the capability to operate both in the grid connected and grid disconnected modes of operation. Therefore, the smooth transition between the modes of operation is achieved here, with the utilization of static transfer switches and appropriate switching of the voltage source converter (VSC) during different modes of operation. The VSC works as a power conditioner unit for mitigating harmonics and providing the reactive power required by the loads. Moreover, power quality problems such as poor power factor, harmonics in the grid current, neutral current etc. are also observed in the distribution network, which pollutes the grid and causes mal-operation of the appliances, increased losses and deterioration in the power factor. Therefore, the control and coordination among various sources are presented here for the integrated system, thereby, complementing the variability of each, along with multifunctional and multimode operating capabilities for the charging of EVs.

This research work aims at the design, control and implementation of various renewable energy sources based microgrids with applications to EVs charging system. The microgrids structures and control algorithms are simulated in MATLAB platform and the simulation results are verified with the test results to be in compliance with the IEEE standards. In order to deal with the power quality issues along with charging of EVs, various configurations are developed, which are classified based on the type of distribution networks i.e. number of power stages, the functionalities of the microgrids and connection of the battery storage to the DC link along with DC/ AC charging capabilities of EVs. Moreover, the three-phase microgrids are further classified into the three-phase three-wire and three-phase four-wire configurations, where the three-phase four-wire microgrids are also capable of providing neutral current compensation abilities. Therefore, the selection of the type of microgrid, depends on the requirements of the consumers. Thus, the control techniques are developed for the renewable energy sources based microgrids with satisfactory operation under the grid connected and grid outage modes of operation along with the uninterrupted power supply to the critical local loads. Moreover, the participation of EVs in the microgrids, has the potential to enhance the system resilience along with the improvement in environmental conditions. Thus, the proficiency in the charging of EVs with the off-board and on-board chargers are tested during various conditions of grid disconnection, load perturbation, varying solar insolation and changing wind speed conditions.

सारांश

यह काम हाइब्रिड वितरित ऊर्जा संसाधनों जैसे सौर, पवन, बैटरी और ईंधन सेल स्रोतों पर आधारित माइक्रोग्रिड के उपयोग पर केंद्रित है, जिसमें इलेक्ट्रिक वाहनों) ईवी (चार्जिंग बुनियादी ढांचे के अनुप्रयोग हैं। माइक्रोग्रिड का उपयोग उपयोगिता ग्रिड के साथ तालमेल बिठाने की क्षमता के साथ-साथ दूरस्थ क्षेत्रों के विद्युतीकरण से संबंधित समस्याओं का समाधान करता है। इस प्रकार, अक्षय ऊर्जा स्रोतों और ऊर्जा भंडारण उपकरणों के उपयोग से, जीवाश्म-ईंधन की खपत में कमी के साथ-साथ दूरस्थ स्थानों को खिलाने की समस्याओं का समाधान किया जा सकता है। इसके अलावा, चार्जिंग उद्देश्यों के लिए माइक्रोग्रिड से जुड़े ईवी, अतिरिक्त भंडारण क्षमता के साथ अत्यधिक लचीले भार के रूप में कार्य करते हैं और हानिकारक उत्सर्जन में कमी के लाभ प्रदान करते हैं, जिससे पर्यावरण के अनुकूल परिवहन की गारंटी मिलती है। सौर पीवी सरणी, पवन टरबाइन और ईंधन सेल स्टैक जैसे नवीकरणीय ऊर्जा स्रोतों से युक्त माइक्रोग्रिड का उपयोग यहां किया जाता है, जो स्थानीय भार में बिजली हस्तांतरण और ईवी की चार्जिंग के साथ-साथ उपयोगिता ग्रिड के साथ तालमेल में काम करते हैं। इसके अलावा, माइक्रोग्रिड विश्वसनीयता ग्रिड से जुड़े और ग्रिड डिस्कनेक्टेड मोड दोनों में संचालित करने की क्षमता पर निर्भर है। इसलिए, संचालन के विभिन्न तरीकों के दौरान स्थिर हस्तांतरण स्विच और वोल्टेज स्रोत कनवर्टर) वीएससी (के उपयुक्त स्विचिंग के उपयोग के साथ, संचालन के तरीकों के बीच सुचारू संक्रमण यहां प्राप्त किया जाता है। वीएससी हार्मोनिक्स को कम करने और भार के लिए आवश्यक प्रतिक्रियाशील शक्ति प्रदान करने के लिए एक पावर कंडीशनर इकाई के रूप में काम करता है। इसके अलावा, बिजली की गुणवत्ता की समस्याएं जैसे कि खराब पावर फैक्टर, ग्रिड करंट में हार्मोनिक्स, न्यूट्रल करंट आदि भी वितरण नेटवर्क में देखे जाते हैं, जो ग्रिड को प्रदूषित करते हैं और उपकरणों के खराब संचालन का कारण बनते हैं, नुकसान में वृद्धि और पावर फैक्टर में गिरावट का कारण बनते हैं। . इसलिए, एकीकृत प्रणाली के लिए विभिन्न स्रोतों के बीच नियंत्रण और समन्वय यहां प्रस्तुत किया गया है, जिससे ईवीएस की चार्जिंग

के लिए बहुआयामी और मल्टीमोड ऑपरेटिंग क्षमताओं के साथ-साथ प्रत्येक की परिवर्तनशीलता का पूरक है। इस शोध कार्य का उद्देश्य ईवीएस चार्जिंग सिस्टम के अनुप्रयोगों के साथ विभिन्न अक्षय ऊर्जा स्रोतों पर आधारित माइक्रोग्रिड का डिजाइन, नियंत्रण और कार्यान्वयन करना है। माइक्रोग्रिड संरचनाएं और नियंत्रण एल्गोरिदम MATLAB प्लेटफॉर्म में सिमुलेटेड हैं और सिमुलेशन परिणाम IEEE मानकों के अनुपालन में परीक्षण परिणामों के साथ सत्यापित किए जाते हैं। ईवी की चार्जिंग के साथ-साथ बिजली की गुणवत्ता के मुद्दों से निपटने के लिए, विभिन्न विन्यास विकसित किए जाते हैं, जिन्हें वितरण नेटवर्क के प्रकार के आधार पर वर्गीकृत किया जाता है, जैसे कि बिजली के चरणों की संख्या, माइक्रोग्रिड की कार्यक्षमता और डीसी से बैटरी भंडारण का कनेक्शन। ईवीएस की डीसी/एसी चार्जिंग क्षमताओं के साथ लिंक। इसके अलावा, तीन-चरण माइक्रोग्रिड को आगे तीन-चरण तीन-तार और तीन-चरण चार-तार कॉन्फिगरेशन में वर्गीकृत किया जाता है, जहां तीन-चरण चार-तार माइक्रोग्रिड भी तटस्थ वर्तमान मुआवजा क्षमता प्रदान करने में सक्षम हैं। इसलिए, माइक्रोग्रिड के प्रकार का चयन उपभोक्ताओं की आवश्यकताओं पर निर्भर करता है। इस प्रकार, महत्वपूर्ण स्थानीय भार के लिए निर्बाध बिजली आपूर्ति के साथ-साथ ग्रिड से जुड़े और ग्रिड आउटेज मोड के संचालन के तहत संतोषजनक संचालन के साथ अक्षय ऊर्जा स्रोतों पर आधारित माइक्रोग्रिड के लिए नियंत्रण तकनीक विकसित की जाती है। इसके अलावा, माइक्रोग्रिड में इलेक्ट्रिक वाहनों की भागीदारी में पर्यावरणीय परिस्थितियों में सुधार के साथ-साथ सिस्टम के लचीलेपन को बढ़ाने की क्षमता है। इस प्रकार, ऑफ-बोर्ड और ऑन-बोर्ड चार्जर्स के साथ इलेक्ट्रिक वाहनों को चार्ज करने में दक्षता का परीक्षण ग्रिड डिस्कनेक्शन, लोड गड़बड़ी, अलग-अलग सौर सूर्यातप और बदलती हवा की गति की स्थितियों की विभिन्न स्थितियों के दौरान किया जाता है।

TABLE OF CONTENTS

	Page No.
Certificate	i
Acknowledgement	ii-iii
Abstract	iv-vii
Table of Contents	viii-xxvii
List of Figures	xviii-xl
List of Tables	xli
List of Abbreviations	xlii
List of Symbols	xlii-xliv
CHAPTER-I INTRODUCTION	1-11
1.1 General	1
1.2 State of Art	3
1.2.1 Power Quality Improvement in Distributed Microgrids	3
1.2.2 Seamless Transition between Off-Grid and Grid Interfaced System	4
1.2.3 Renewable Energy Sources Based Microgrids	5
1.2.4 Electric Vehicle Charging Infrastructure	6
1.3 Objectives and Scope of Work	7
1.4 Outline of Chapters	9
CHAPTER-II LITERATURE REVIEW	12-34
2.1 General	12
2.2 Literature Survey	12
2.2.1 Review on Control of Grid Interfaced Solar PV System	13
2.2.2 Review on Renewable Energy Sources Based Microgrids	14
2.2.3 Review on Control of Fuel Cells and Wind Power Based Distribution Generation System	17
2.2.4 Review on Microgrids Based EV Chargers and Charging Infrastructure	19
2.3 Identified Research Areas	20
2.4 Conclusions	21
CHAPTER-III DESIGN AND DEVELOPMENT OF MULTIPURPOSE THREE-PHASE SOLAR PV SYSTEM WITH GRID SYNCHRONIZATION	23-65
3.1 General	23
3.2 Configurations and Operating Principle of Three-Phase Grid Interfaced Solar PV System	24
3.2.1 Single Stage PV System Interfaced to the Three-Phase Grid	24
3.2.2 Double Stage PV System Interfaced to the Three-Phase Grid	24
3.3 Design of Grid Interfaced Three-Phase Solar PV System	25
3.3.1 Single Stage PV System Interfaced to the Three-Phase Grid	25
3.3.2 Double Stage PV System Interfaced to the Three-Phase Grid	26
3.4 Control Algorithms for Three-Phase Grid Interfaced Solar PV System	26
3.4.1 Control Approach for Single Stage PV System Interfaced to Three-Phase Grid	27

3.4.1.1	MPPT Control Algorithm for Single-Stage PV System Interfaced to Three-Phase Grid	28
3.4.1.2	Operation with Grid Interconnection for Single-Stage PV System Interfaced to Three-Phase Grid	28
3.4.1.3	Operation during Grid Disconnection for Single-Stage PV System Interfaced to Three-Phase Grid	32
3.4.1.4	Synchronization Control of Single-Stage PV System Interfaced to Three-Phase Grid	32
3.4.2	Control Approach for Double Stage PV System Interfaced to Three-Phase Grid	33
3.4.2.1	Grid Connected Mode of Operation of Double-Stage PV System Interfaced to Three-Phase Grid	34
3.4.2.2	Control for Double-Stage PV System Interfaced to Three-Phase Grid during Standalone Mode of Operation	36
3.4.2.3	Synchronization Control of Double-Stage PV System Interfaced to Three-Phase Grid	36
3.5	MATLAB Based Modeling of Three-Phase Solar PV System Interfaced to Three-Phase Grid	37
3.5.1	MATLAB Based Modeling of Single Stage PV System Interfaced to Three-Phase Grid	37
3.5.2	MATLAB Based Modeling of Double Stage PV System Interfaced to Three-Phase Grid	37
3.6	Hardware Implementation of Three-Phase Solar PV System Interfaced to Three-Phase Grid	38
3.6.1	Hardware Configuration of OPAL-RT (OP4510) controller	39
3.6.2	Interfacing Circuit for Hall Effect Current Sensors	40
3.6.3	Interfacing Circuit for Hall Effect Voltage Sensors	41
3.6.4	Interfacing Circuit for Gate Driver	42
3.7	Results and Discussion	43
3.7.1	Performance of Single-Stage PV System Interfaced to Three-Phase Grid	43
3.7.1.1	Simulated Performance of Single-Stage PV System Interfaced to Three-Phase Grid	44
3.7.1.1.1	Simulated Performance of Single-Stage PV System Interfaced to Three-Phase Grid during Intermittent Solar Insolation Condition	44
3.7.1.1.2	Simulated Performance of Single-Stage PV System Interfaced to Three-Phase Grid during Dynamic Loading Condition	45
3.7.1.1.3	Simulated Performance of Single-Stage PV System Interfaced to Three-Phase Grid during Conversion from Grid Interconnected to Grid Outage Modes of operation	46
3.7.1.1.4	Simulated Performance of Single-Stage PV System Interfaced to Three-Phase Grid during Conversion from Grid Outage to Grid Interconnected Modes of operation	47
3.7.1.2	Experimental Performance of Single-Stage PV System Interfaced to Three-Phase Grid	49
3.7.1.2.1	Experimental Performance of Single-Stage PV System Interfaced to Three-Phase Grid during Steady State Operation	50
3.7.1.2.2	Experimental Performance of Single-Stage PV System	52

	Interfaced to Three-Phase Grid during Variable Solar Insolation and Load Unbalancing Conditions	
3.7.1.2.3	Experimental Performance of Single-Stage PV System Interfaced to Three-Phase Grid during Transition between Grid Connected and Disconnected Modes of Operation	53
3.7.2	Performance of Double-Stage PV System Interfaced to Three-Phase Grid	54
3.7.2.1	Simulated Performance of Double-Stage PV System Interfaced to Three-Phase Grid	55
3.7.2.1.1	Harmonic Analysis of Double-Stage PV System Interfaced to Three-Phase Grid	55
3.7.2.1.2	Simulated Performance of Double-Stage PV System Interfaced to Three-Phase Grid during Change between Grid Interconnection and Disconnection Modes of Operation	56
3.7.2.1.3	Simulated Performance of Double-Stage PV System Interfaced to Three-Phase Grid during Load Removal and Varying Solar Insolation Conditions	58
3.7.2.2	Experimental Performance of Double-Stage PV System Interfaced to Three-Phase Grid	60
3.7.2.2.1	Experimental Performance of Double-Stage Solar PV System Interfaced to Three-Phase Grid at Steady-State Condition	61
3.7.2.2.2	Experimental Performance of Double-Stage Solar PV System Interfaced to the Three-Phase Grid during Mode Transition between Grid Connected and Disconnected Modes of Operation	63
3.7.2.2.3	Experimental Performance of Double-Stage Solar PV System Interfaced to the Three-Phase Grid during Load Perturbation Condition	64
3.7.2.2.4	Experimental Performance of Double-Stage Solar PV System Interfaced to the Three-Phase Grid during Variable Solar Irradiation Condition	65
3.8	Conclusions	66
CHAPTER-IV	DESIGN AND DEVELOPMENT OF MULTIPURPOSE THREE-PHASE FOUR-WIRE SOLAR PV SYSTEM WITH GRID SYNCHRONIZATION	67-109
4.1	General	67
4.2	Configurations and Operating Principle of Three-Phase Four-Wire Grid Interfaced Solar PV System	67
4.2.1	Single Stage PV System Interfaced to the Three-Phase Four-Wire Grid	68
4.2.2	Double Stage PV System Interfaced to the Three-Phase Four-Wire Grid	68
4.3	Design of Grid Interfaced Three-Phase Four-Wire Solar PV System	69
4.3.1	Single Stage PV System Interfaced to the Three-Phase Four-Wire Grid	69
4.3.2	Double Stage PV System Interfaced to the Three-Phase Four-Wire Grid	70
4.4	Control Algorithms for Three-Phase Four-Wire Grid Interfaced Solar PV System	71
4.4.1	Control Approach for Single Stage PV System Interfaced to Three-Phase Four-Wire Grid	71
4.4.1.1	Operation with Grid Interconnection for Single-Stage PV System Interfaced to Three-Phase Four-Wire Grid	71

4.4.1.2	Islanded/ Grid Disconnected Mode of Operation of Three-Phase Four-Wire Single-Stage PV System	76
4.4.1.3	Synchronization Control of Single-Stage PV System Interfaced to Three-Phase Four-Wire Grid	77
4.4.2	Control Approach for Double Stage PV System Interfaced to Three-Phase Four-Wire Grid	78
4.4.2.1	Grid Connected Mode of Operation of Double-Stage PV System Interfaced to Three-Phase Four-Wire Grid	78
4.4.2.2	Voltage Control during Grid Outage Mode of Operation of Double-Stage PV System Interfaced to Three-Phase Four-Wire Grid	82
4.4.2.3	Synchronization Control of Double-Stage PV System Interfaced to Three-Phase Four-Wire Grid	82
4.5	MATLAB Based Modeling of Three-Phase Four-Wire Solar PV System Interfaced to Utility Grid	83
4.5.1	MATLAB Based Modeling of Single Stage PV System Interfaced to Three-Phase Four-Wire Grid	83
4.5.2	MATLAB Based Modeling of Double Stage PV System Interfaced to Three-Phase Three-Four Grid	84
4.6	Hardware Implementation of Three-Phase Four-Wire Solar PV System Interfaced to Utility Grid	84
4.6.1	Hardware Configuration of OPAL-RT (OP4510) Controller	85
4.6.2	Interfacing Circuit for Hall Effect Current Sensors	85
4.6.3	Interfacing Circuit for Hall Effect Voltage Sensors	86
4.6.4	Interfacing Circuit for Gate Driver	86
4.7	Results and Discussion	86
4.7.1	Performance of Single-Stage PV System Interfaced to the Three-Phase Four-Wire Grid	87
4.7.1.1	Simulated Performance of Single-Stage PV System Interfaced to the Three-Phase Four-Wire Grid	87
4.7.1.1.1	Simulated Performance of Single-Stage PV System Interfaced to Three-Phase Four-Wire Grid at Intermittent PV Radiation	87
4.7.1.1.2	Simulated Performance of Single-Stage PV System Interfaced to the Three-Phase Four-Wire Grid during Dynamic Loading Condition	88
4.7.1.1.3	Simulated Performance of Single-Stage PV System Interfaced to the Three-Phase Four-Wire Grid during Transition from Grid Interconnected to Grid Outage Modes of Operation	89
4.7.1.1.4	Simulated Performance of Single-Stage PV System Interfaced to the Three-Phase Four-Wire Grid during Transition from Grid Outage to Grid Interconnected Modes of Operation	90
4.7.1.2	Experimental Performance of Single-Stage PV System Interfaced to the Three-Phase Four-Wire Grid	92
4.7.1.2.1	Experimental Performance of Single-Stage PV System Interfaced to the Three-Phase Four-Wire Grid during Steady-State Condition	92
4.7.1.2.2	Experimental Performance of Single-Stage PV System Interfaced to the Three-Phase Four-Wire Grid during Mode	94

	Change from Grid Connected to Disconnected Modes of Operation	
4.7.1.2.3	Experimental Performance of Single-Stage PV System Interfaced to the Three-Phase Four-Wire Grid during Mode Change from Grid Disconnected to Connected Operation of Single-Stage PV System Interfaced to the Three-Phase Four-Wire Grid	95
4.7.1.2.4	Experimental Performance of Single-Stage PV System Interfaced to the Three-Phase Four-Wire Grid during Load Unbalancing Condition	96
4.7.1.2.5	Experimental Performance of Single-Stage PV System Interfaced to the Three-Phase Four-Wire Grid during Load Unbalancing Condition during Variable Solar Irradiation Condition	97
4.7.2	Performance of Double-Stage PV System Interfaced to Three-Phase Four-Wire Grid	98
4.7.2.1	Simulated Performance of Double-Stage PV System Interfaced to Three-Phase Four-Wire Grid	98
4.7.2.1.1	Simulated Performance of Double-Stage PV System Interfaced to the Three-Phase Four-Wire Grid during Transition between Grid Interconnection and Disconnection Modes of Operation	98
4.7.2.1.2	Simulated Performance of Double-Stage PV System Interfaced to the Three-Phase Four-Wire Grid during Load Unbalancing Condition	100
4.7.2.1.3	Simulated Performance of Double-Stage PV System Interfaced to the Three-Phase Four-Wire Grid during Variable Solar Insolation Condition	101
4.7.2.1.4	Harmonic Analysis of Double-Stage PV System Interfaced to the Three-Phase Four-Wire Grid	102
4.7.2.2	Experimental Performance of Double-Stage PV System Interfaced to the Three-Phase Four-Wire Grid	103
4.7.2.2.1	Experimental Performance of Double-Stage PV System Interfaced to the Three-Phase Four-Wire Grid at Steady-State Condition	104
4.7.2.2.2	Experimental Performance of Double-Stage PV System Interfaced to the Three-Phase Four-Wire Grid during Transition from Grid Presence to Outage Mode of Operation	106
4.7.2.2.3	Experimental Performance of Double-Stage PV System Interfaced to the Three-Phase Four-Wire Grid during Transition from Grid Outage to Grid Presence Mode of Operation	107
4.7.2.2.4	Experimental Performance of Double-Stage PV System Interfaced to the Three-Phase Four-Wire Grid during Dynamic Loading Condition	107
4.7.2.2.5	Experimental Performance of Double-Stage PV System Interfaced to the Three-Phase Four-Wire Grid during Varying Solar Irradiation Condition	108
4.8	Conclusions	109

**CHAPTER-V DESIGN AND DEVELOPMENT OF THREE-PHASE
SOLAR PV-BES SYSTEM UNDER GRID 110-165
DISTURBANCES**

5.1	General	110
5.2	Configurations and Operating Principle of Three-Phase Grid Interfaced Solar PV-BES System	110
5.2.1	Double Stage PV-BES System Integrated to Three-Phase Grid	111
5.2.2	Double Stage PV-BES System Integrated to Three-Phase Grid with Bidirectional Converter Controlled BES	111
5.2.3	Single Stage PV-BES System Integrated to Three-Phase Grid with Bidirectional Converter Controlled BES	112
5.3	Design of Three-Phase Solar PV-BES Grid Interfaced Solar PV-BES System	113
5.3.1	Design of Double-Stage PV-BES System Integrated to Three-Phase Grid	113
5.3.2	Double-Stage PV-BES System Integrated to Three-Phase Grid with Bidirectional Converter Controlled BES	
5.3.3	Single-Stage PV-BES System Integrated to Three-Phase Grid with Bidirectional Converter Controlled BES	114
5.4	Control Algorithms for Three-Phase Grid Interfaced Solar PV-BES System	115
5.4.1	Control Approach for Double-Stage PV-BES System Integrated to Three-Phase Grid	115
5.4.1.1	Operation with Grid Interconnection for Double-Stage PV-BES System Integrated to Three-Phase Grid	116
5.4.1.2	Operation during Grid Outage for Double-Stage PV-BES System Integrated to Three-Phase Grid	118
5.4.1.3	Synchronization Control for Double-Stage PV-BES System Integrated to Three-Phase Grid	120
5.4.2	Control Approach for Double-Stage PV-BES System with Bidirectional Converter Controlled BES	120
5.4.2.1	Operation with Grid Interconnection for Double-Stage PV-BES System with Bidirectional Converter Controlled BES	121
5.4.2.2	Operation with Grid Disconnection for Double-Stage PV-BES System with Bidirectional Converter Controlled BES	124
5.4.2.3	Synchronization Control for Double-Stage PV-BES System with Bidirectional Converter Controlled BES	124
5.4.3	Control Approach for Single-Stage PV-BES System with Bidirectional Converter Controlled BES	124
5.4.3.1	Operation with Grid Connection for Single-Stage PV-BES System with Bidirectional Converter Controlled BES	125
5.4.3.2	Operation with Grid Disconnection for Single-Stage PV-BES System with Bidirectional Converter Controlled BES	128
5.4.3.3	Synchronization Control for Single-Stage PV-BES System with Bidirectional Converter Controlled BES	128
5.5	MATLAB Based Modeling of Three-Phase Grid Interfaced Solar PV-BES System	128
5.5.1	MATLAB Based Modeling of Grid Interfaced Double Stage PV-BES System	129
5.5.2	MATLAB Based Modeling of Grid Interfaced Double Stage PV-BES System with Bidirectional Converter Controlled BES	129
5.5.3	MATLAB Based Modeling of Grid Interfaced Single Stage PV-BES System with Bidirectional Converter	130

5.6 Hardware Implementation of Three-Phase Solar PV-BES System Interfaced with Utility Grid	130
5.6.1 Hardware Configuration of OPAL-RT (OP4510) Controller	131
5.6.2 Interfacing Circuit for Hall Effect Current Sensors	131
5.6.3 Interfacing Circuit for Hall Effect Voltage Sensors	131
5.6.4 Interfacing Circuit for Gate Driver	131
5.7 Results and Discussion	132
5.7.1 Performance of Double Stage PV-BES System Integrated to Three-Phase Grid	132
5.7.1.1 Simulated Performance of Double-Stage PV-BES System Integrated to Three-Phase Grid	132
5.7.1.1.1 Simulated Performance of Double-Stage PV-BES System Integrated to Three-Phase Grid during Transition from Grid Connected to Disconnected Mode of Operation	132
5.7.1.1.2 Simulated Performance of Double-Stage PV-BES System Integrated to Three-Phase Grid during Transition from Grid Disconnected to Connected Mode of Operation	133
5.7.1.1.3 Simulated Performance of Double-Stage PV-BES System Integrated to Three-Phase Grid with Power Quality Enhancement during Weak Grid Conditions Including Load Variability and Erratic Solar Insolation	134
5.7.1.2 Experimental Performance of Double-Stage PV-BES System Integrated to Three-Phase Grid	137
5.7.1.2.1 Experimental Performance of Double-Stage PV-BES System Integrated to Three-Phase Grid during Constant Power Feeding Mode of Operation	138
5.7.1.2.2 Experimental Performance of Three-Phase Grid Integrated Double-Stage PV-BES System during Standalone Mode of Operation	139
5.7.1.2.3 Experimental Performance of Double-Stage PV-BES System Integrated to Three-Phase Grid during Transition from Grid Connected to Disconnected Mode of Operation	140
5.7.1.2.4 Experimental Performance of Double-Stage PV-BES System Integrated to Three-Phase Grid during Transition from Grid Disconnected to Connected Mode of Operation	140
5.7.1.2.5 Experimental Performance of double-stage PV-BES system integrated to three-phase grid during Variable solar insolation condition	141
5.7.1.2.6 Experimental Performance of Double-Stage PV-BES System Integrated to Three-Phase Grid at Load Unbalancing Condition	142
5.7.2 Performance of Double-Stage PV-BES System Integrated to Three-Phase Grid with Bidirectional Converter Controlled BES	143
5.7.2.1 Simulated Performance of Double-Stage PV-BES System Integrated to Three-Phase Grid with Bidirectional Converter Controlled BES	143
5.7.2.1.1 Simulated Performance of Double-Stage PV-BES System Integrated to Three-Phase Grid with Bidirectional Converter Controlled BES at Intermittent PV Radiation	144
5.7.2.1.2 Simulated Performance of Double-Stage PV-BES System Integrated to Three-Phase Grid with Bidirectional	144

	Converter Controlled BES during Dynamic Loading Condition	
5.7.2.1.3	Simulated Performance of Double-Stage PV-BES System Integrated to Three-Phase Grid with Bidirectional Converter Controlled BES during Transition from Grid Interconnected to Grid Outage Mode of Operation	145
5.7.2.1.4	Simulated Performance of Double-Stage PV-BES System Integrated to Three-Phase Grid with Bidirectional Converter Controlled BES during Transition from Grid Interconnected to Grid Outage Modes of Operation	146
5.7.2.2	Experimental Performance of Double Stage PV-BES System Integrated to Three-Phase Grid with Bidirectional Converter Controlled BES	148
5.7.2.2.1	Experimental Performance of Double-Stage PV-BES System Integrated to Three-Phase Grid with Bidirectional Converter Controlled BES during Transition from Grid Interconnected to Grid Outage Mode of Operation	148
5.7.2.2.2	Experimental Performance of Double-Stage PV-BES System Integrated to Three-Phase Grid with Bidirectional Converter Controlled BES during Transition from Grid Outage to Grid Connected Mode of Operation	149
5.7.2.2.3	Experimental Performance of Double-Stage PV-BES System Integrated to Three-Phase Grid with Bidirectional Converter Controlled BES during Variable Solar Insolation Condition	150
5.7.2.2.4	Experimental Performance of Double-Stage PV-BES System Integrated to Three-Phase Grid with Bidirectional Converter Controlled BES at Load Unbalancing Condition	151
5.7.2.2.5	Experimental Performance of Double-Stage PV-BES System Integrated to Three-Phase Grid with Bidirectional Converter Controlled BES at Constant Power Feeding Mode of Operation	152
5.7.2.2.6	Experimental Performance of Double-Stage PV-BES System Integrated to Three-Phase Grid with Bidirectional Converter Controlled BES during Standalone Mode of Operation	153
5.7.3	Performance of Single-Stage PV-BES System Integrated to Three-Phase Grid with Bidirectional Converter Controlled BES	154
5.7.3.1	Simulated Performance of Single Stage PV-BES System Integrated to Three-Phase Grid with Bidirectional Converter	154
5.7.3.1.1	Simulated Performance of Single-Stage PV-BES System Integrated to Three-Phase Grid with Bidirectional Converter Controlled BES during Mode Change from Grid Connected to Grid Disconnected Operation	154
5.7.3.1.2	Simulated Performance of Single-Stage PV-BES System Integrated to Three-Phase Grid with Bidirectional Converter Controlled BES during Mode Change from Grid Disconnected to Grid Connected Operation	155

5.7.3.1.3	Simulated Performance of Single-Stage PV-BES System Integrated to Three-Phase Grid with Bidirectional Converter Controlled BES during Variable Solar Insolation Condition	156
5.7.3.1.4	Simulated Performance of Single-Stage PV-BES System Integrated to Three-Phase Grid with Bidirectional Converter Controlled BES during Load Removal Condition	157
5.7.3.2	Experimental Performance of Single Stage PV-BES System Integrated to Three-Phase Grid with Bidirectional Converter Controlled BES	159
5.7.3.2.1	Experimental Performance of Single-Stage PV-BES System Integrated to Three-Phase Grid with Bidirectional Converter Controlled BES during Transition from Grid Interconnected to Grid Outage Mode of Operation	160
5.7.3.2.2	Experimental Performance of Single-Stage PV-BES System Integrated to Three-Phase Grid with Bidirectional Converter Controlled BES during Mode Change from Grid Outage to Grid Connected Mode of Operation	161
5.7.3.2.3	Experimental Performance of Single-Stage PV-BES System Integrated to Three-Phase Grid with Bidirectional Converter Controlled BES during Weak Grid Conditions Including Erratic Solar Insolation and Load Variability	162
5.7.3.2.4	Experimental Performance of Single-Stage PV-BES System Integrated to Three-Phase Grid with Bidirectional Converter Controlled BES during Constant Power Feeding Mode of Operation	163
5.7.3.2.5	Experimental Performance of Single-Stage PV-BES System Integrated to Three-Phase Grid with Bidirectional Converter Controlled BES during Standalone Mode of Operation	164
5.8	Conclusions	165
CHAPTER-VI	DESIGN AND DEVELOPMENT OF THREE-PHASE FOUR-WIRE SOLAR PV-BES SYSTEM UNDER GRID DISTURBANCES	166-225
6.1	General	166
6.2	Configurations and Operating Principle of Three-Phase Four-Wire Solar PV-BES Grid Interfaced Solar PV System	167
6.2.1	Double Stage PV-BES System Integrated to Three-Phase Four-Wire Grid	167
6.2.2	Double-Stage PV-BES System Integrated to Three-Phase Four-Wire Grid with Bidirectional Converter Controlled BES	167
6.2.3	Single-Stage PV-BES System Integrated to Three-Phase Four-Wire Grid with Bidirectional Converter Controlled BES	168
6.3	Design of Three-Phase Four-Wire Grid Interfaced Solar PV BES System	169
6.3.1	Double Stage PV-BES System Integrated to Three-Phase Four-Wire Grid	169
6.3.2	Double-Stage PV-BES System Integrated to Three-Phase Four-Wire Grid with Bidirectional Converter Controlled BES	170
6.3.3	Single-Stage PV-BES System Integrated to Three-Phase Four-Wire Grid with Bidirectional Converter Controlled BES	171
6.4	Control Algorithms for Grid Interfaced Three-Phase Four-Wire Solar PV-BES System	171

6.4.1	Control Approach for Double Stage PV-BES System Integrated to Three-Phase Four-Wire Grid	172
6.4.1.1	Operation with Grid Interconnection for Double-Stage PV-BES System Integrated to Three-Phase Grid	172
6.4.1.2	Operation of Double-Stage PV-BES System Integrated to Three-Phase Four-Wire Grid during Grid Outage Mode of Operation	175
6.4.1.3	Synchronization Control of Double-Stage PV-BES System Integrated to Three-Phase Four-Wire Grid	176
6.4.2	Control Approach for Double-Stage PV-BES System Integrated to Three-Phase Four-Wire Grid with Bidirectional Converter Controlled BES	177
6.4.2.1	Operation of Double-Stage PV-BES System Integrated to Three-Phase Four-Wire Grid with Bidirectional Converter Controlled BES during Grid Connected Mode of Operation	178
6.4.2.2	Control of Double-Stage PV-BES System with Bidirectional Converter Controlled BES Integrated to Three-Phase Four-Wire Grid during Standalone Mode of Operation	181
6.4.2.3	Synchronization Control of Double-Stage PV-BES System with Bidirectional Converter Controlled BES Integrated to Three-Phase Four-Wire Grid	181
6.4.3	Control Approach for Single-Stage PV-BES System Integrated to Three-Phase Four-Wire Grid with Bidirectional Converter Controlled BES	181
6.4.3.1	Control of Single-Stage PV-BES System Integrated to Three-Phase Four-Wire Grid with Bidirectional Converter Controlled BES during Grid Connected Mode of Operation	182
6.4.3.2	Control of Single-Stage PV-BES System with Bidirectional Converter Controlled BES during Grid Disconnection Mode of Operation	185
6.4.3.3	Synchronization Control for Single-Stage PV-BES System with Bidirectional Converter Controlled BES	185
6.5	MATLAB Based Modeling of Grid Interfaced Three-Phase Four-Wire Solar PV-BES System	185
6.5.1	MATLAB Based Modeling of Double Stage PV-BES System Integrated to Three-Phase Four-Wire Grid	186
6.5.2	MATLAB Based Modeling of Double-Stage PV-BES System Integrated to Three-Phase Four-Wire Grid with Bidirectional Converter Controlled BES	186
6.5.3	MATLAB Based Modeling of Single-Stage PV-BES System Integrated to Three-Phase Four-Wire Grid with Bidirectional Converter Controlled BES	187
6.6	Hardware Implementation of Three-Phase Four-Wire Solar PV-BES System	188
6.6.1	Hardware Configuration of OPAL-RT (OP4510) Controller	188
6.6.2	Interfacing Circuit for Hall Effect Current Sensors	188
6.6.3	Interfacing Circuit for Hall Effect Voltage Sensors	188
6.6.4	Interfacing Circuit for Gate Driver	188
6.7	Results and Discussion	189
6.7.1	Performance of Double Stage PV-BES System Integrated to Three-Phase Four-Wire Grid	189
6.7.1.1	Simulated Performance of Double Stage PV-BES System Integrated to Three-Phase Four-Wire Grid	189

6.7.1.1.1	Simulated Performance of Double-Stage PV-BES System Integrated to Three-Phase Four-Wire Grid during Transition from Grid Connected to Disconnected Mode of Operation	189
6.7.1.1.2	Simulated Performance of Double-Stage PV-BES System Integrated to Three-Phase Four-Wire Grid during Transition from Grid Disconnected to Connected Mode of Operation	190
6.7.1.1.3	Simulated Performance of Double-Stage PV-BES System Integrated to Three-Phase Four-Wire Grid with Enhancement of Power Quality during Weak Grid Conditions Including Load Variability and Erratic Solar Insolation	191
6.7.1.2	Experimental Performance of Double-Stage PV-BES System Integrated to Three-Phase Four-Wire Grid	194
6.7.1.2.1	Experimental Performance of Double-Stage PV-BES System Integrated to Three-Phase Four-Wire Grid during Transition from Grid Connected to Grid Disconnected Modes of Operation	195
6.7.1.2.2	Experimental Performance of Double-Stage PV-BES System Integrated to Three-Phase Four-Wire Grid during Transition from Grid Disconnected to Grid Connected Modes of Operation	196
6.7.1.2.3	Experimental Performance of Double-Stage PV-BES System Integrated to Three-Phase Four-Wire Grid at Load Removal Condition	196
6.7.1.2.4	Experimental Performance of Double-Stage PV-BES System Integrated to Three-Phase Four-Wire Grid at Variable Solar Insolation Condition	197
6.7.1.2.5	Experimental Performance of Double-Stage PV-BES System Integrated to Three-Phase Four-Wire Grid during Constant Power Feeding Mode of Operation	198
6.7.1.2.6	Experimental Performance of Three-Phase Four-Wire Double-Stage PV-BES System during Standalone Mode of Operation	200
6.7.2	Performance of Double Stage PV-BES System with Bidirectional Converter Controlled BES Integrated to Three-Phase Four-Wire Grid	201
6.7.2.1	Simulated Performance of Double-Stage PV-BES System Integrated to Three-Phase Four-Wire Grid with Bidirectional Converter Controlled BES	201
6.7.2.1.1	Simulated Performance of Double-Stage PV-BES System Integrated to Three-Phase Four-Wire Grid with Bidirectional Converter Controlled BES during Transition from Grid Connected to Grid Outage Modes of Operation	201
6.7.2.1.2	Simulated Performance of Double-Stage PV-BES System Integrated to Three-Phase Four-Wire Grid with Bidirectional Converter Controlled BES during Transition from Grid Connected to Grid Outage Modes of Operation	202
6.7.2.1.3	Simulated Performance of Double-Stage PV-BES System with Bidirectional Converter Controlled BES Integrated to Three-Phase Four-Wire Grid with Enhancement of Power	204

	Quality during Weak Grid Conditions Including Erratic Solar Insolation and Load Variability	
6.7.2.2	Experimental Performance of Double-Stage PV-BES System with Bidirectional Converter Controlled BES Integrated to Three-Phase Four-Wire Grid	206
6.7.2.2.1	Experimental Performance of Double-Stage PV-BES System with Bidirectional Converter Controlled BES Integrated to Three-Phase Four-Wire Grid during Constant Power Feeding Mode of Operation	207
6.7.2.2.2	Experimental Performance of Three-Phase Four-Wire Double-Stage PV-BES System with Bidirectional Converter Controlled BES during Standalone Mode of Operation	208
6.7.2.2.3	Experimental Performance of Double-Stage PV-BES System Integrated to Three-Phase Four-Wire Grid with Bidirectional Converter Controlled BES during Transition from Grid Connected to Grid Outage Modes of Operation	209
6.7.2.2.4	Experimental Performance of Double-Stage PV-BES System Integrated to Three-Phase Four-Wire Grid with Bidirectional Converter Controlled BES during Transition from Grid Outage to Grid Connected Modes of Operation	210
6.7.2.2.5	Experimental Performance of Double-Stage PV-BES System Integrated to Three-Phase Four-Wire Grid with Bidirectional Converter Controlled BES at Load Unbalancing Condition	211
6.7.2.2.6	Experimental Performance of Double-Stage PV-BES System Integrated to Three-Phase Four-Wire Grid with Bidirectional Converter Controlled BES at Variable Solar Insolation Condition	212
6.7.3	Performance of Single-Stage PV-BES System Integrated to Three-Phase Four-Wire Grid with Bidirectional Converter Controlled BES	213
6.7.3.1	Simulated Performance of Single-Stage PV-BES System Integrated to Three-Phase Four-Wire Grid with Bidirectional Converter Controlled BES	213
6.7.3.1.1	Simulated performance of Single-Stage PV-BES System Integrated to Three-Phase Four-Wire Grid with Bidirectional Converter Controlled BES during Mode Change between Grid Connected to Grid Disconnected Operation	214
6.7.3.1.2	Simulated performance of Single-Stage PV-BES System Integrated to Three-Phase Four-Wire Grid with Bidirectional Converter Controlled BES during Mode Change between Grid Connected to Grid Disconnected Operation	215
6.7.3.1.3	Simulated Performance of Single-Stage PV-BES System Integrated to Three-Phase Four-Wire Grid with Bidirectional Converter Controlled BES at Dynamic Loading Condition	216
6.7.3.1.4	Simulated Performance of Single-Stage PV-BES System Integrated to Three-Phase Four-Wire Grid with	217

	Bidirectional Converter Controlled BES at Variable Solar Insolation Condition	
6.7.3.2	Experimental Performance of Single-Stage PV-BES System Integrated to Three-Phase Four-Wire Grid with Bidirectional Converter Controlled BES	219
6.7.3.2.1	Experimental Performance of Single-Stage PV-BES System Integrated to Three-Phase Four-Wire Grid with Bidirectional Converter Controlled BES during Mode Change from Grid Connected to Grid Disconnected Operation	219
6.7.3.2.2	Experimental Performance of Single-Stage PV-BES System Integrated to Three-Phase Four-Wire Grid with Bidirectional Converter Controlled BES during Mode Change from Grid Disconnected to Grid Connected Operation	220
6.7.3.2.3	Experimental Performance of Single-Stage PV-BES System Integrated to Three-Phase Four-Wire Grid with Bidirectional Converter Controlled BES at Load Unbalancing Condition	221
6.7.3.2.4	Experimental Performance of Single-Stage PV-BES System Integrated to Three-Phase Four-Wire Grid with Bidirectional Converter Controlled BES at Variable Solar Insolation Condition	222
6.7.3.2.5	Experimental Performance of Single-Stage PV-BES System Integrated to Three-Phase Four-Wire Grid with Bidirectional Converter Controlled BES at Constant Power Feeding Mode of Operation	223
6.7.3.2.6	Experimental Performance of Single-Stage PV-BES System Integrated to Three-Phase Four-Wire Grid with Bidirectional Converter Controlled BES during Standalone Mode of Operation	224
6.8	Conclusions	225
CHAPTER-VII	DESIGN AND DEVELOPMENT OF MULTIPLE PVs WITH BATTERY FOR ELECTRIC VEHICLES BY DC/AC CHARGING	226-270
7.1	General	226
7.2	Configurations of Multiple PVs Interfaced with Three-Phase Grid for DC/AC Charging of Electric Vehicles	226
7.2.1	Multiple PVs Based DC Charging of EVs Interfaced with Three-Phase Grid	227
7.2.2	Multiple PVs Based AC Charging of EVs Interfaced with Three-Phase Grid	227
7.3	Design of Multiple PV Arrays Interfaced with Three-Phase Grid For DC/AC Charging of Electric Vehicles	228
7.3.1	Design of Multiple PVs System Interfaced with Three-Phase Grid for DC Charging of EVs	228
7.3.2	Design of Multiple PVs System Interfaced with Three-Phase Grid for AC Charging of EVs	229
7.4	Control Algorithms of Multiple PV Arrays Interfaced with Three-Phase Grid for DC/AC Charging of Electric Vehicles	230

7.4.1 Control Approach for Multiple PVs Interfaced with Three-Phase Grid for DC Charging of EVs	231
7.4.1.1 Grid Connected Control of Multiple PVs for DC Charging of EVs	231
7.4.1.2 Standalone Control of Multiple PVs for DC Charging of EVs	235
7.4.1.3 Synchronization Control of Multiple PVs for DC Charging of EVs	236
7.4.2 Control Approach of Multiple PV Arrays Interfaced with Three-Phase Grid for AC Charging of EVs	238
7.4.2.1 Control for Voltage Source Converter (VSC ₁) of Multiple PV Arrays Interfaced with Three-Phase Grid for AC Charging of EVs	238
7.4.2.2 Control for Voltage Source Converter (VSC ₂) of Multiple PVs Interfaced with Three-Phase Grid for AC Charging of EVs	242
7.4.2.3 Synchronization Control of Multiple PVs Interfaced with Three-Phase Grid for AC Charging of EVs	244
7.5 MATLAB Based Modeling of Multiple PV Arrays Interfaced with Three-Phase Grid for DC/AC Charging of Electric Vehicles	244
7.5.1 MATLAB Based Modelling of Multiple PV Arrays Interfaced with Three-Phase Grid for DC Charging of EVs	244
7.5.2 MATLAB Based Modelling of Multiple PVs Interfaced with Three-Phase Grid for AC Charging of EVs	245
7.6 Results and Discussion	246
7.6.1. Performance of Multiple PV Arrays interfaced with Three-Phase Grid for DC Charging of EVs	246
7.6.1.1 Simulated Performance of Multiple PV Arrays interfaced with Three-Phase Grid for DC charging of EVs	246
7.6.1.1.1 Simulated Performance of Multiple PV Arrays interfaced with Three-Phase Grid for DC charging of EVs during Mode Change between Grid Connection and Disconnection	246
7.6.1.1.2 Simulated Behaviour of Multiple PV Arrays interfaced with Three-Phase Grid for DC charging of EVs during Weak Grid Conditions Including Load Variability and Erratic Solar Insolation	249
7.6.1.2 Hardware in Loop Implementation of Multiple PVs Interfaced with Three-Phase Grid for DC Charging of Electric Vehicles	251
7.6.1.2.1 Harmonic Analysis of Multiple PV Arrays Interfaced with Three-Phase Grid for DC Charging of Electric Vehicles	252
7.6.1.2.2 Performance of Multiple PV Arrays Interfaced with Three-Phase Grid for DC Charging of Electric Vehicles during Mode Transition from Grid Connected to Disconnected Modes of Operation	253
7.6.1.2.3 Performance of Multiple PV Arrays Interfaced with Three-Phase Grid for DC Charging of Electric Vehicles during Mode Transition from Grid Disconnected to Connected Modes of Operation	255
7.6.1.2.4 Performance of Multiple PVs Interfaced with Three-Phase Grid for DC Charging of Electric Vehicles during Load Unbalancing Condition	256
7.6.1.2.5 Performance of Multiple PV Arrays Interfaced with Three-Phase Grid for DC Charging of Electric Vehicles during Variable Solar Insolation Condition	257

7.6.2	Performance of Multiple PV Arrays Interfaced with Three-Phase Grid for AC Charging of EVs	258
7.6.2.1	Simulated Performance of Multiple PVs interfaced with Three-Phase Grid for AC Charging of EVs	258
7.6.2.1.1	Simulated Performance of Transition from Grid Connected to Disconnected Mode of Operation Multiple PV Arrays Interfaced with Three-Phase Grid for AC Charging of EVs	259
7.6.2.1.2	Simulated Performance of Multiple PV Arrays Interfaced with Three-Phase Grid for AC Charging of EVs during Transition from Grid Disconnected to Connected Mode of Operation	260
7.6.2.1.3	Simulated Performance of Multiple PV Arrays Interfaced with Three-Phase Grid for AC Charging of EVs during Load Unbalancing Condition	261
7.6.2.1.4	Simulated Performance of Multiple PV Arrays Interfaced with Three-Phase Grid for AC Charging of EVs during Variable Solar Insolation Condition	262
7.6.2.2	Hardware in Loop Implementation of Multiple PV Arrays Interfaced with Three-Phase Grid for AC Charging of Electric Vehicles	263
7.6.2.2.1	Performance of Multiple PV Arrays Interfaced with Three-Phase Grid for AC Charging of Electric Vehicles during Mode Transition from Grid Connected to Disconnected Modes of Operation	264
7.6.2.2.2	Performance of Multiple PV Arrays Interfaced with Three-Phase Grid for AC Charging of Electric Vehicles during Mode Transition from Grid Disconnected to Connected Modes of Operation	266
7.6.2.2.3	Performance of Multiple PV Arrays Interfaced with Three-Phase Grid for AC Charging of Electric Vehicles during Load Unbalancing Condition	267
7.6.2.2.4	Performance of Multiple PV Arrays Interfaced with Three-Phase Grid for AC Charging of Electric Vehicles during Variable Solar Insolation Condition	268
7.7	Conclusions	269
CHAPTER-VIII	DESIGN AND DEVELOPMENT OF DISTRIBUTED MICROGRIDS CONSISTING OF SOLAR, WIND, BATTERY AND FUEL CELL SOURCES BASED COMMON DC BUS EV CHARGING	271-320
8.1	General	271
8.2	Configurations and Operating Principle of Common DC Bus EV Charging Infrastructure with Distributed Microgrids	272
8.2.1	Common DC Bus Charging with Distributed Microgrids Consisting of Solar, Battery and Fuel Cell Sources	272
8.2.2	Common DC Bus Charging with Distributed Microgrids Consisting of Solar, Wind, Battery and Fuel Cell Sources	273
8.3	Design of Common DC Bus EV Charging Infrastructure with Distributed Microgrids	274
8.3.1	Common DC Bus Charging with Distributed Microgrids Consisting of Solar, Battery and Fuel Cell Sources	274

8.3.2	Common DC Bus Charging with Distributed Microgrids Consisting of Solar, Wind, Battery and Fuel Cell Sources	275
8.4	Control Algorithms for Distributed Microgrids with Common DC Bus EV Charging	276
8.4.1	Control Algorithms for Common DC Bus EV Charging with Distributed Microgrids Consisting of Solar, Battery and Fuel Cell Sources	277
8.4.1.1	Control Algorithm for Grid-Tied Common DC Bus Charging of EVs with Distributed Microgrid Consisting of Solar, Battery and Fuel Cell Sources	277
8.4.1.2	Control Algorithm for Standalone Mode of Operation for Common DC Bus Charging of EVs with Distributed Microgrid Consisting of Solar, Battery and Fuel Cell Sources	281
8.4.1.3	Synchronization Control for Common DC Bus Charging of EVs with Distributed Microgrid Consisting of Solar, Battery and Fuel Cell Sources	283
8.4.2	Control Approach for Common DC Bus EV Charging with Distributed Microgrids Consisting of Solar, Wind, Battery and Fuel Cell Sources	284
8.4.2.1	Grid-Tied Control Technique for Common DC Bus EV Charging with Distributed Microgrid Consisting of Solar, Wind, Battery and Fuel Cell Sources	284
8.4.2.2	Standalone Control Technique for Common DC Bus EV Charging with Distributed Microgrid Consisting of Solar, Wind, Battery and Fuel Cell Sources	288
8.4.2.3	Synchronization Control Technique for Common DC Bus EV Charging with Distributed Microgrid Consisting of Solar, Wind, Battery and Fuel Cell Sources	288
8.5	MATLAB Based Modelling of Distributed Microgrids with Common DC Bus EV Charging	288
8.5.1	MATLAB Based Modeling of Common DC Bus Charging with Distributed Microgrids Consisting of Solar, Battery and Fuel Cell Sources	289
8.5.2	MATLAB Based Modeling of Common DC Bus Charging with Distributed Microgrids Consisting of Solar, Wind, Battery and Fuel Cell Sources	289
8.6	Results and Discussion	290
8.6.1	Performance of Common DC Bus EVs Charging with Distributed Microgrid Consisting of Solar, Battery and Fuel Cell Sources	290
8.6.1.1	Simulated Performance of Common DC Bus EVs Charging with Distributed Microgrid Consisting of Solar, Battery and Fuel Cell Sources	291
8.6.1.1.1	Simulated Performance of Mode Change between Grid Connection to Disconnection for Common DC Bus EVs Charging with Distributed Microgrid Consisting of Solar, Battery and Fuel Cell Sources	291
8.6.1.1.2	Simulated Performance of Mode Change between Grid Disconnection to Connection for Common DC Bus EVs Charging with Distributed Microgrid Consisting of Solar, Battery and Fuel Cell Sources	291
8.6.1.1.3	Simulated Behaviour of Common DC Bus EVs Charging with Distributed Microgrid Consisting of Solar, Battery and Fuel Cell Sources for Variation in charging of EVs during Grid Connected/ Disconnected Modes of Operation	292

8.6.1.1.4	Simulated Behaviour during Weak Grid Conditions Including Load Variability and Erratic Solar Insolation for Common DC Bus EVs Charging with Distributed Microgrid Consisting of Solar, Battery and Fuel Cell Sources	294
8.6.1.2	Hardware in Loop Implementation of Common DC Bus EVs Charging with Distributed Microgrid Consisting of Solar, Battery and Fuel Cell Sources	297
8.6.1.2.1	Performance of Common DC Bus EVs Charging with Distributed Microgrid Consisting of Solar, Battery and Fuel Cell Sources during Mode Transition from Grid Connected to Disconnected Condition	297
8.6.1.2.2	Performance of Common DC Bus EVs Charging with Distributed Microgrid Consisting of Solar, Battery and Fuel Cell Sources during Mode Transition from Grid Disconnected to Connected Condition	298
8.6.1.2.3	Performance of Common DC Bus Charging with Distributed Microgrid Consisting of Solar, Battery and Fuel Cell Sources for Variation in Charging of EVs during Transition between Grid Connected and Disconnected Modes of Operation	300
8.6.1.2.4	Improvement of Power Quality (PQ) During Weak Grid Conditions along with EVs Charging Capability with Distributed Microgrid Consisting of Solar, Battery and Fuel Cell Sources	301
8.6.1.2.5	Performance of Common DC Bus Charging with Distributed Microgrid Consisting of Solar, Battery and Fuel Cell Sources during Constant Grid Power Feeding Mode of Operation	304
8.6.2	Performance of Common DC Bus Charging of EVs with Distributed Microgrid Consisting of Solar, Wind, Battery and Fuel Cell Sources	305
8.6.2.1	Simulated Performance of Common DC Bus EVs Charging with Distributed Microgrid Consisting of Solar, Wind, Battery and Fuel Cell Sources	305
8.6.2.1.1	Simulated Performance of Common DC Bus EVs Charging with Distributed Microgrid Consisting of Solar, Wind, Battery and Fuel Cell Sources during Mode Change between Grid Connection to Disconnection	306
8.6.2.1.2	Simulated Performance of Common DC Bus EVs Charging with Distributed Microgrid Consisting of Solar, Wind, Battery and Fuel Cell Sources during Mode Change between Grid Disconnection to Connection	307
8.6.2.1.3	Simulated Performance of Common DC Bus EVs Charging with Distributed Microgrid Consisting of Solar, Wind, Battery and Fuel Cell Sources during Load Removal Condition	308
8.6.2.1.4	Simulated Performance of Common DC Bus EVs Charging with Distributed Microgrid Consisting of Solar, Wind, Battery and Fuel Cell Sources during Constant Grid Power Feeding During Wind Speed Variation Condition	309

8.6.2.1.5	Simulated Performance of Common DC Bus EVs Charging with Distributed Microgrid Consisting of Solar, Wind, Battery and Fuel Cell Sources during Variable Solar Insolation Condition	310
8.6.2.2	Hardware in Loop Implementation of Common DC Bus EVs Charging with Distributed Microgrid Consisting of Solar, Wind, Battery and Fuel Cell Sources	311
8.6.2.2.1	Performance of Common DC Bus Charging of EVs with Distributed Microgrid Consisting of Solar, Wind, Battery and Fuel Cell Sources during Mode Transition from Grid Connected to Disconnected Condition	312
8.6.2.2.2	Performance of Common DC Bus Charging of EVs with Distributed Microgrid Consisting of Solar, Wind, Battery and Fuel Cell Sources during Mode Transition from Grid Disconnected to Grid Connected Mode of Operation	314
8.6.2.2.3	Performance of Common DC Bus EVs Charging with Distributed Microgrid Consisting of Solar, Wind, Battery and Fuel Cell Sources during Load Removal Condition	316
8.6.2.2.4	Performance of Common DC Bus EVs Charging with Distributed Microgrid Consisting of Solar, Wind, Battery and Fuel Cell Sources during Solar Insolation Variation Condition	317
8.6.2.2.5	Performance of Common DC Bus EVs Charging with Distributed Microgrid Consisting of Solar, Wind and Fuel Cell Sources during Constant Grid Power Feeding Wind Speed Variation Condition	318
8.7	Conclusions	319
CHAPTER-IX	DESIGN AND DEVELOPMENT OF DISTRIBUTED MICROGRIDS CONSISTING OF SOLAR, WIND, BATTERY AND FUEL CELL SOURCES BASED COMMON AC BUS EV CHARGING	321-364
9.1	General	321
9.2	Configurations and Operating Principle of Common AC Bus EV Charging Infrastructure with Distributed Microgrids	322
9.2.1	Common AC Bus Charging with Distributed Microgrids Consisting of Solar, Battery and Fuel Cell Sources	322
9.2.2	Common AC Bus Charging with Distributed Microgrids Consisting of Solar, Wind, Battery and Fuel Cell Sources	322
9.3	Design of Common AC Bus EV Charging Infrastructure with Distributed Microgrids	323
9.3.1	Common AC Bus Charging with Distributed Microgrids Consisting of Solar, Battery and Fuel Cell Sources	323
9.3.2	Common AC Bus Charging with Distributed Microgrids Consisting of Solar, Wind, Battery and Fuel Cell Sources	324
9.4	Control Algorithms for Distributed Microgrids with Common AC Bus Charging of EVs	325
9.4.1	Control for Grid Connected Solar PV Array Interfaced Voltage Source Converter (VSC ₁) for Common AC Bus Charging of EVs	326
9.4.2	Control for Grid Connected Fuel Cell Stack Interfaced Voltage Source Converter (VSC ₂) for Common AC Bus Charging of EVs	329

9.4.3	Control for Grid Connected PMSG Driven Wind Turbine Interfaced Voltage Source Converter (VSC ₃) for Common AC Bus Charging of EVs	331
9.4.4	Constant Grid Power Feeding Mode for Grid Connected Common AC Bus EV Charging with Distributed Microgrids Consisting of Solar, Wind, Battery and Fuel Cell Sources	333
9.4.5	Standalone Control Technique for Common AC Bus EV Charging with Distributed Microgrids Consisting of Solar, Wind, Battery and Fuel Cell Sources	334
9.4.6	Synchronization Control for Common AC Bus EV Charging with Distributed Microgrids Consisting of Solar, Wind, Battery and Fuel Cell Sources	335
9.5	MATLAB Based Distributed Microgrids with Common AC Bus EV Charging	336
9.5.1	MATLAB Based Modeling of Common AC Bus Charging with Distributed Microgrids Consisting of Solar, Battery and Fuel Cell Sources	336
9.5.2	MATLAB Based Modeling of Common AC Bus Charging with Distributed Microgrids Consisting of Solar, Wind, Battery and Fuel Cell Sources	337
9.6	Results and Discussion	338
9.6.1	Performance of Common AC Bus Charging with Distributed Microgrids Consisting of Solar, Battery and Fuel Cell Sources	338
9.6.1.1	Simulated Performance of Common AC Bus Charging with Distributed Microgrids Consisting of Solar, Battery and Fuel Cell Sources during Mode Transition between Grid Connected and Disconnected Modes of Operation	338
9.6.1.2	Simulated Performance of Common AC Bus Charging with Distributed Microgrids Consisting of Solar, Battery and Fuel Cell Sources during Weak Grid Conditions Including Variable Solar Insolation, Load Removal for	340
9.6.1.3	Simulated Performance of Common AC Bus Charging with Distributed Microgrids Consisting of Solar, Battery and Fuel Cell Sources during Constant Grid Power Feeding Mode of Operation	342
9.6.1.4	Hardware in Loop Implementation of Common AC Bus Charging of EVs with Distributed Microgrids Consisting of Solar, Battery and Fuel Cell Sources	344
9.6.1.4.1	Performance of Common AC Bus Charging of EVs with Distributed Microgrids Consisting of Solar, Battery and Fuel Cell Sources during Mode Transition from Grid Connected to Disconnected Condition	345
9.6.1.4.2	Performance of Common AC Bus Charging of EVs with Distributed Microgrids Consisting of Solar, Battery and Fuel Cell Sources during Mode Transition from Grid Disconnected to Connected Condition	346
9.6.1.4.3	Performance of Common AC Bus Charging with Distributed Microgrids Consisting of Solar, Battery and Fuel Cell Sources during Weak Grid Conditions Including Load Removal and Variable Solar Insolation	347
9.6.1.4.4	Performance of Common AC Bus Charging of EVs with Distributed Microgrids Consisting of Solar, Battery and Fuel Cell Sources during Constant Grid Power Feeding Mode of Operation	350

9.6.2 Performance of Common AC Bus Charging with Distributed Microgrids Consisting of Solar, Wind, Battery and Fuel Cell Sources	350
9.6.2.1 Simulated Performance of Mode Transition between Grid Disconnection to Connection for Common AC Bus Charging with Distributed Microgrids Consisting of Solar, Wind, Battery and Fuel Cell Sources	351
9.6.2.2 Simulated Performance of Mode Change between Grid Disconnection to Connection for Common AC Bus EVs Charging with Distributed Microgrids Consisting of Solar, Wind, Battery and Fuel Cell Sources	353
9.6.2.3 Simulated Performance of Variable Solar Insolation Condition for Common AC Bus EVs Charging with Distributed Microgrids Consisting of Solar, Wind, Battery and Fuel Cell Sources	354
9.6.2.4 Simulated Performance of Load Removal Condition for Common AC Bus EVs Charging with Distributed Microgrids Consisting of Solar, Wind, Battery and Fuel Cell Sources	355
9.6.2.5 Simulated Performance of Constant Grid Power Feeding During Wind Speed Variation Condition for Common AC Bus Charging of EVs with Distributed Microgrids Consisting of Solar, Wind, Battery and Fuel Cell Sources	356
9.6.2.6 Hardware in Loop Implementation of Common AC Bus Charging of EVs with Distributed Microgrids Consisting of Solar, Wind, Battery and Fuel Cell Sources	357
9.6.2.6.1 Performance of Common AC Bus Charging of EVs with Distributed Microgrids Consisting of Solar, Wind, Battery and Fuel Cell Sources during Mode Transition from Grid Connected to Disconnected Mode of Operation	357
9.6.2.6.2 Performance of Common AC Bus Charging of EVs with Distributed Microgrids Consisting of Solar, Wind and Fuel Cell Sources during Mode Transition from Grid Disconnected to Connected Condition	360
9.6.2.6.3 Performance of Common AC Bus Charging of EVs with Distributed Microgrids Consisting of Solar, Wind, Battery and Fuel Cell Sources during Load Removal Conditions	361
9.6.2.6.4 Performance of Common AC Bus Charging of EVs with Solar Insolation Variation with Distributed Microgrids Consisting of Solar, Wind, Battery and Fuel Cell Sources	362
9.6.2.6.5 Performance of Common AC Bus Charging of EVs with Distributed Microgrids Consisting of Solar, Wind, Battery and Fuel Cell Sources for Constant Grid Power Feeding During Wind Speed Variation Condition	363
9.7 Conclusions	364
CHAPTER-X	
MAIN CONCLUSIONS AND SUGGESTIONS FOR FURTHER WORK	365-370
10.1 General	365
10.2 Main Conclusions	366
10.3 Suggestions for Further Work	369
REFERENCES	371-378
LIST OF PUBLICATIONS	379-381

LIST OF FIGURES

- Fig. 3.1 Circuit configuration of single-stage PV system interfaced to the three-phase grid
- Fig. 3.2 Circuit configuration of double-stage PV system interfaced to the three-phase grid
- Fig. 3.3 Control algorithm based on adaptive digital filter for grid interfaced single-stage solar PV system
- Fig. 3.4 Control mechanism of double-stage solar PV system interfaced to three-phase grid during grid connected mode of operation
- Fig. 3.5 Control mechanism for boost converter associated with double-stage solar PV system
- Fig. 3.6 Performance of double-stage PV system interfaced to three-phase grid during grid outage mode of operation
- Fig. 3.7 MATLAB model of single-stage PV system interfaced to the three-phase grid
- Fig. 3.8 MATLAB model of double-stage PV system interfaced to the three-phase grid
- Fig. 3.9 Components required for hardware implementation of grid interfaced three-phase solar PV system
- Fig. 3.10 Laboratory prototype
- Fig. 3.11 OPAL-RT OP4510 I/O Blocks and Configuration
- Fig. 3.12 Schematic for current sensor board
- Fig. 3.13 Photograph of current sensor
- Fig. 3.14 Schematic for voltage sensor board
- Fig. 3.15 Photograph of voltage sensor
- Fig. 3.16 Schematic of opto-isolation board
- Fig. 3.17 Photograph of opto-isolators
- Fig. 3.18 (a)-(b) Simulated performance of single-stage PV system interfaced to three-phase grid during intermittent solar insolation condition
- Fig. 3.19 (a)-(b) Simulated performance of grid connected mode of single-stage PV system interfaced to three-phase grid during dynamic loading condition
- Fig. 3.20 (a)-(b) Simulated performance of single-stage PV system interfaced to three-phase grid during transition from grid interconnected to grid outage modes of operation
- Fig. 3.21 (a)-(b) Simulated performance of single-stage PV system interfaced to three-phase grid during transition from grid outage to grid interconnected modes of operation
- Fig. 3.22 (a)-(c) Harmonic analysis of grid interfaced single-stage PV system (a) load current (b) grid current (c) load voltage
- Fig. 3.23 (a)-(b) Experimental performance of single-stage PV system during (a) grid connected and (b) grid outage modes of operation.
- Fig. 3.24 (a)-(h) Steady state operation of single-stage PV System interfaced to the three-phase grid
- Fig. 3.25 (a)-(c) Experimental performance of single-stage PV System during grid outage during steady state operation
- Fig. 3.26 (a)-(f) Experimental performance of single-stage PV system interfaced to three-phase grid during conditions of variable solar insolation and load unbalancing
- Fig. 3.27 (a)-(d) Experimental performance of single-stage PV system interfaced to three-phase grid during mode change between grid outage and grid connected modes of operation
- Fig. 3.28 (a)-(b) Experimental performance of single-stage PV system interfaced to three-phase grid during mode change from grid outage to grid connected modes of operation

- Fig. 3.29 (a)-(c) Harmonic analysis of grid interfaced double-stage PV system (a) load current (b) grid current (c) load voltage
- Fig. 3.30 (a)-(b) Simulated performance of double-stage PV system interfaced to three-phase grid during conversion from grid connected to grid outage modes of operation
- Fig. 3.31 (a)-(b) Simulated performance of double-stage PV system interfaced to three-phase grid during conversion from grid outage to grid connected modes of operation
- Fig. 3.32 (a)-(b) Simulated performance of double-stage PV system interfaced to three-phase grid during load removal conditions
- Fig. 3.33 (a)-(b) Simulated performance of double-stage PV system interfaced to three-phase grid during variable solar insolation conditions
- Fig. 3.34 (a)-(b) Experimental performance of MPPT for double-stage PV system during (a) grid connected and (b) grid outage modes of operation.
- Fig. 3.35 (a)-(i) Experimental performance of grid connected double-stage solar PV system at steady state operation
- Fig. 3.36 (a)-(d) Experimental performance of grid disconnected double-stage solar PV system at steady state operation
- Fig. 3.37 (a)-(d) Experimental performance of double-stage solar PV system interfaced with three-phase grid during transition from grid connected to disconnected modes of operation
- Fig. 3.38 (a)-(d) Experimental performance of double-stage solar PV system interfaced with three-phase grid during transition from grid disconnected to grid connected modes of operation
- Fig.3.39 (a)-(d) Experimental performance of grid interfaced double-stage solar PV system during load removal condition
- Fig.3.40 (a)-(d) Experimental performance of double-stage solar PV system at steady-state during variable solar insolation condition
- Fig. 4.1 Circuit configuration of single-stage PV system interfaced to the three-phase four-wire grid
- Fig. 4.2 Circuit configuration of double-stage PV system interfaced to the three-phase four-wire grid
- Fig. 4.3 Control Structure during grid connection/disconnection of single-stage PV system interfaced with three-phase four-wire grid
- Fig. 4.4 Control algorithm of adaptive transversal filter with leaky integrator for of single-stage PV system interfaced with three-phase four-wire grid
- Fig. 4.5 Control mechanism during grid availability of double-stage PV system interfaced to three-phase four-wire grid
- Fig. 4.6 Grid unavailability control technique of double-stage PV system interfaced to three-phase four-wire grid
- Fig. 4.7 MATLAB model for three-phase four wire grid interfaced single-stage solar PV system
- Fig. 4.8 MATLAB model for three-phase four wire grid interfaced double-stage solar PV system
- Fig. 4.9 Laboratory prototype of three-phase four-wire grid interfaced solar PV system
- Fig. 4.10 (a)-(b) Simulated performance of single-stage PV system interfaced to the three-phase four-wire grid during intermittent solar insolation condition
- Fig. 4.11 (a)-(b) Simulated performance of grid connected mode of single-stage PV system interfaced to the three-phase four-wire grid during dynamic loading condition
- Fig. 4.12 (a)-(b) Simulated performance of grid connected mode of single-stage PV system interfaced to the three-phase four-wire grid during transition from grid interconnected to grid outage modes of operation

- Fig. 4.13 (a)-(b) Simulated performance of grid connected mode of single-stage PV system interfaced to the three-phase four-wire grid during transition from grid outage to grid interconnected modes of operation
- Fig. 4.14 (a)-(c) Harmonic spectra of load current (i_{La}), grid current (i_{La}) and load voltage (v_{La}) of single-stage PV system interfaced to the three-phase four-wire grid
- Fig. 4.15 (a)-(b) Experimental performance of single-stage PV system interfaced to the three-phase four-wire grid during (a) grid connected and (b) grid disconnected modes of operation
- Fig. 4.16 (a)-(h) Experimental performance of single-stage PV system interfaced to the three-phase four-wire grid during steady-state condition
- Fig. 4.17 (a)-(c) Experimental performance of grid disconnected three-phase four-wire single-stage PV system during steady-state condition
- Fig. 4.18 (a)-(d) Experimental performance of single-stage PV system interfaced to the three-phase four-wire grid during mode change from grid connected to disconnected modes of operation
- Fig. 4.19 (a)-(d) Experimental performance of single-stage PV system interfaced to the three-phase four-wire grid during mode change from grid disconnected to connected modes of operation
- Fig. 4.20 (a)-(d) Experimental performance of single-stage PV system interfaced to the three-phase four-wire grid during load unbalancing condition
- Fig. 4.21 (a)-(d) Experimental performance of single-stage PV system interfaced to the three-phase four-wire grid during variable solar irradiation condition
- Fig. 4.22 (a)-(d) Simulated performance of double-stage PV system interfaced to the three-phase four-wire grid during mode transition from grid connected to disconnected modes of operation
- Fig. 4.23 (a)-(b) Simulated performance of double-stage PV system interfaced to the three-phase four-wire grid during mode transition from grid disconnected to connected modes of operation
- Fig. 4.24 (a)-(b) Simulated performance of double-stage PV system interfaced to the three-phase four-wire grid during dynamic loading condition
- Fig. 4.25 (a)-(b) Simulated performance of double-stage PV system interfaced to the three-phase four-wire grid during variable insolation condition
- Fig. 4.26 (a)-(c) Enhancement of PQ of double-stage PV system interfaced to the three-phase four-wire grid
- Fig. 4.27 (a)-(b) MPPT performance during solar insolation of 1000 W/m² of double-stage PV system interfaced to the three-phase four-wire grid
- Fig. 4.28 (a)-(h) Experimental performance of double-stage PV system interfaced to the three-phase four-wire grid at steady-state condition
- Fig. 4.29 (a)-(c) Experimental performance of standalone three-phase four-wire double-stage PV system at steady-state condition
- Fig. 4.30 (a)-(d) Experimental performance of double-stage PV system interfaced to the three-phase four-wire grid during mode change from grid connected to disconnected modes of operation
- Fig. 4.31 (a)-(d) Experimental performance of double-stage PV system interfaced to the three-phase four-wire grid during mode change from grid disconnected to connected modes of operation
- Fig. 4.32 (a)-(c) Experimental performance of double-stage PV system interfaced to the three-phase four-wire grid during dynamic loading condition
- Fig. 4.33 (a)-(b) Experimental performance of double-stage PV system interfaced to the three-phase four-wire grid during variable solar insolation condition

- Fig. 5.1 Double-stage PV-BES system integrated to three-phase grid feeding critical loads
- Fig. 5.2 Double-stage PV-BES system integrated to three-phase grid with bidirectional converter feeding local loads
- Fig. 5.3 Single-stage PV-BES system integrated to three-phase grid with bidirectional converter feeding local loads
- Fig. 5.4 Control Structure during grid connection/disconnection of double stage PV-BES system integrated to three-phase grid
- Fig. 5.5 Control Structure during grid connection of double-stage PV-BES system with bidirectional converter controlled BES
- Fig. 5.6 Control Structure during grid outage mode of operation of double-stage PV-BES system with bidirectional converter controlled BES
- Fig. 5.7 Control Structure during grid connection of single-stage PV-BES system with bidirectional converter controlled BES
- Fig. 5.8 Control Structure during grid outage mode of operation of single-stage PV-BES system with bidirectional converter controlled BES
- Fig. 5.9 Control structure of bidirectional converter controlled BES of single-stage PV-BES system
- Fig. 5.10 MATLAB model for grid interfaced double-stage PV-BES system
- Fig. 5.11 MATLAB model for grid interfaced double-stage PV-BES system with bidirectional converter controlled BES
- Fig. 5.12 MATLAB model for grid interfaced single-stage PV-BES system with bidirectional converter controlled BES
- Fig. 5.13 (a)-(b) Simulated performance of double-stage PV-BES system integrated to three-phase grid during transition from grid interconnected to grid outage mode of operation
- Fig. 5.14 (a)-(b) Simulated performance of double-stage PV-BES system integrated to three-phase grid during transition from grid outage to grid interconnected mode of operation
- Fig. 5.15 (a)-(b) Simulated performance of double-stage PV-BES system integrated to three-phase grid during dynamic loading condition
- Fig. 5.16 (a)-(b) Simulated performance of double-stage PV-BES system integrated to three-phase grid during variable solar insolation condition
- Fig. 5.17 (a)-(c) Harmonic spectra of load current (i_{La}), grid current (i_{La}) and load voltage (v_{La}) of double-stage PV-BES system integrated to three-phase grid
- Fig. 5.18 (a)-(b) Performance of MPPT for solar insolation of (a) 1000 W/m² (b) 700 W/m² of double-stage PV-BES system integrated to three-phase grid
- Fig. 5.19 (a)-(j) Experimental performance of double-stage PV-BES system integrated to three-phase grid during constant power feeding mode of operation
- Fig. 5.20 (a)-(e) Experimental performance of of double-stage PV-BES system during standalone mode of operation
- Fig. 5.21 (a)-(d) Experimental performance of double-stage PV-BES system integrated to three-phase grid during transition from grid interconnected to grid outage mode of operation
- Fig. 5.22 (a)-(d) Experimental performance of double-stage PV-BES system integrated to three-phase grid during transition from grid outage to grid interconnected mode of operation
- Fig. 5.23 (a)-(c) Experimental performance of double-stage PV-BES system integrated to three-phase grid during variable solar insolation condition
- Fig. 5.24 (a)-(c) Experimental performance of double-stage PV-BES system integrated to three-phase grid during dynamic loading condition

- Fig. 5.25 (a)-(b) Simulated performance of double-stage PV-BES system integrated to three-phase grid with bidirectional converter controlled BES at intermittent solar insolation
- Fig. 5.26 (a)-(b) Simulated performance of double-stage PV-BES system integrated to three-phase grid with bidirectional converter controlled BES during dynamic loading condition
- Fig. 5.27 (a)-(b) Simulated performance of double-stage PV-BES system integrated to three-phase grid with bidirectional converter controlled BES during transition to grid outage mode
- Fig. 5.28 (a)-(b) Simulated performance of double-stage PV-BES system integrated to three-phase grid with bidirectional converter controlled BES during transition to grid connected mode
- Fig. 5.29 (a)-(c) Harmonic analysis of double-stage PV-BES system integrated to three-phase grid with bidirectional converter controlled BES
- Fig. 5.30 (a)-(b) Performance of MPPT for solar insolation of (a) 1000 W/m² (b) 800 W/m² of double-stage PV-BES system integrated to three-phase grid with bidirectional converter controlled BES
- Fig. 5.31 (a)-(c) Experimental Performance of double-stage PV-BES system integrated to three-phase grid with bidirectional converter controlled BES during mode change from grid connected to disconnected modes of operation
- Fig. 5.32 (a)-(c) Experimental performance of double-stage PV-BES system integrated to three-phase grid with bidirectional converter controlled BES during mode change from grid connected to disconnected mode of operation
- Fig. 5.33 (a)-(b) Experimental performance of double-stage PV-BES system integrated to three-phase grid with bidirectional converter controlled BES during variable solar insolation condition
- Fig. 5.34 (a)-(c) Experimental performance of double-stage PV-BES system integrated to three-phase grid with bidirectional converter controlled BES at load removal condition
- Fig. 5.35 (a)-(j) Experimental performance of double-stage PV-BES system integrated to three-phase grid at constant power feeding mode
- Fig. 5.36 (a)-(e) Experimental performance of standalone mode of operation of double-stage PV-BES system integrated to three-phase grid with bidirectional converter controlled BES
- Fig. 5.37 (a)-(b) Simulated performance of single-stage PV-BES system integrated to three-phase grid with bidirectional converter controlled BES during mode change from grid connected to disconnected mode of operation
- Fig. 5.38 (a)-(b) Simulated performance of single-stage PV-BES system integrated to three-phase grid with bidirectional converter controlled BES during mode change from grid disconnected to connected mode of operation
- Fig. 5.39 (a)-(b) Simulated performance of single-stage PV-BES system integrated to three-phase grid with bidirectional converter controlled BES at variable solar insolation condition
- Fig. 5.40 (a)-(b) Simulated performance of single-stage PV-BES system integrated to three-phase grid with bidirectional converter controlled BES during load unbalancing condition
- Fig. 5.41 (a)-(c) Harmonic analysis of single-stage PV-BES system integrated to three-phase grid with bidirectional converter controlled BES

- Fig. 5.42 (a)-(b) Experimental performance of MPPT for solar insolation of (a) 1000 W/m² (b) 800 W/m² of single-stage PV-BES system integrated to three-phase grid with bidirectional converter controlled BES
- Fig. 5.43 (a)-(d) Experimental performance of single-stage PV-BES system integrated to three-phase grid with bidirectional converter controlled BES during mode change from grid connected to disconnected mode of operation
- Fig. 5.44 (a)-(d) Experimental performance of single-stage PV-BES system integrated to three-phase grid with bidirectional converter controlled BES during mode change from grid disconnected to connected mode of operation
- Fig. 5.45 (a)-(c) Experimental performance of single-stage PV-BES system integrated to three-phase grid with bidirectional converter controlled BES during load removal condition
- Fig. 5.46 (a)-(c) Experimental performance of single-stage PV-BES system integrated to three-phase grid with bidirectional converter controlled BES during variable solar insolation condition
- Fig. 5.47 (a)-(j) Experimental performance of single-stage PV-BES system integrated to three-phase grid with bidirectional converter controlled BES during constant power feeding mode of operation
- Fig. 5.48 (a)-(e) Experimental performance of single-stage PV-BES system integrated to three-phase grid with bidirectional converter controlled BES during standalone mode of operation
- Fig. 6.1 Double-stage PV-BES system integrated to three-phase four-wire grid feeding critical loads
- Fig. 6.2 Double-stage PV-BES system integrated to three-phase four-wire grid with bidirectional converter controlled BES grid feeding local loads
- Fig. 6.3 Single-stage PV-BES system integrated to three-phase four-wire grid with bidirectional converter controlled BES grid feeding local loads
- Fig. 6.4 Control Structure of double stage PV-BES system integrated to three-phase four-wire grid during grid connection mode of operation
- Fig. 6.5 Control Structure of double stage PV-BES system integrated to three-phase four-wire grid during standalone mode of operation
- Fig. 6.6 Control structure of double-stage PV-BES system with bidirectional converter controlled BES during grid connection and grid outage mode of operation
- Fig. 6.7 Control structure of single-stage PV-BES system with bidirectional converter controlled BES during grid connection mode of operation
- Fig. 6.8 Control structure of single-stage PV-BES system with bidirectional converter controlled BES during grid outage mode of operation
- Fig. 6.9 Control mechanism of a bidirectional converter controlled BES of single-stage PV-BES system integrated to three-phase four-wire grid
- Fig.6.10 MATLAB model for three-phase four-wire grid interfaced double-stage PV-BES system
- Fig.6.11 MATLAB model for three-phase four-wire grid interfaced double-stage PV-BES system with bidirectional converter controlled BES
- Fig.6.12 MATLAB model for three-phase four-wire grid interfaced single-stage PV-BES system with bidirectional converter controlled BES
- Fig. 6.13 (a)-(b) Simulated performance of double-stage PV-BES system integrated to three-phase four-wire grid during transition from grid connected to grid outage modes of operation

- Fig. 6.14 (a)-(b) Simulated performance of double-stage PV-BES system integrated to three-phase four-wire grid during transition from grid outage to grid connected modes of operation
- Fig. 6.15 (a)-(b) Simulated performance of double-stage PV-BES system integrated to three-phase four-wire grid at dynamic loading condition
- Fig. 6.16 (a)-(b) Simulated performance of double-stage PV-BES system integrated to three-phase four-wire grid at variable solar insolation condition
- Fig. 6.17 (a)-(c) Harmonic spectra of load current (i_{La}), grid current (i_{La}) and load voltage (v_{La}) of double-stage PV-BES system integrated to three-phase four-wire grid
- Fig. 6.18 (a)-(b) Performance of MPPT of double-stage PV-BES system integrated to three-phase four-wire grid at solar insolation level of (a) 1000 W/m² (b) 800 W/m²
- Fig. 6.19 (a)-(d) Experimental performance of double-stage PV-BES system integrated to three-phase four-wire grid during transition from grid connected to grid outage modes of operation
- Fig. 6.20 (a)-(d) Experimental performance of double-stage PV-BES system integrated to three-phase four-wire grid during transition from grid outage to grid connected modes of operation
- Fig. 6.21 (a)-(c) Experimental performance of double-stage PV-BES system integrated to three-phase four-wire grid at load removal condition
- Fig. 6.22 (a)-(c) Experimental performance of double-stage PV-BES system integrated to three-phase four-wire grid at variable solar insolation condition
- Fig. 6.23 (a)-(i) Experimental performance of double-stage PV-BES system integrated to three-phase four-wire grid during constant power feeding mode of operation
- Fig. 6.24 (a)-(d) Experimental Performance of three-phase four-wire double-stage PV-BES system during standalone mode of operation
- Fig. 6.25 (a)-(b) Simulated performance of double-stage PV-BES system with bidirectional converter controlled BES integrated to three-phase four-wire grid during transition from grid connected to grid outage mode of operation
- Fig. 6.26 (a)-(b) Simulated performance of double-stage PV-BES system with bidirectional converter controlled BES integrated to three-phase four-wire grid during transition from grid outage to grid connected modes of operation
- Fig. 6.27 (a)-(c) Harmonic spectra of load current, grid current and load voltage of double-stage PV-BES system with bidirectional converter controlled BES integrated to three-phase four-wire grid
- Fig. 6.28 (a)-(b) Simulated performance of double-stage PV-BES system with bidirectional converter controlled BES integrated to three-phase four-wire grid at variable solar insolation condition
- Fig. 6.29 (a)-(b) Simulated performance of double-stage PV-BES system with bidirectional converter controlled BES integrated to three-phase four-wire grid at dynamic loading condition
- Fig. 6.30 (a)-(b) Performance of double-stage PV-BES system integrated to three-phase grid with bidirectional converter controlled BES for MPPT with solar insolation of (a) 1000 W/m² (b) 800 W/m²
- Fig. 6.31 (a)-(i) Experimental performance of double-stage PV-BES system with bidirectional converter controlled BES integrated to three-phase four-wire grid during constant power feeding mode of operation
- Fig. 6.32 (a)-(d) Experimental performance of double-stage PV-BES system with bidirectional converter controlled BES integrated to three-phase four-wire grid during standalone mode of operation

- Fig. 6.33 (a)-(d) Experimental performance of double-stage PV-BES system with bidirectional converter controlled BES integrated to three-phase four-wire grid during transition from grid connected to grid disconnected modes of operation
- Fig. 6.34 (a)-(d) Experimental performance of double-stage PV-BES system with bidirectional converter controlled BES integrated to three-phase four-wire grid during transition from grid disconnected to grid connected modes of operation
- Fig. 6.35 (a)-(c) Experimental performance of double-stage PV-BES system with bidirectional converter controlled BES integrated to three-phase four-wire at load unbalancing condition
- Fig. 6.36 (a)-(c) Experimental performance of double-stage PV-BES system with bidirectional converter controlled BES integrated to three-phase four-wire at variable solar insolation condition
- Fig. 6.37 (a)-(b) Simulated performance of single-stage PV-BES system with bidirectional converter controlled BES integrated to three-phase four-wire grid during transition from grid connected to grid outage modes of operation
- Fig. 6.38 (a)-(b) Simulated performance of single-stage PV-BES system with bidirectional converter controlled BES integrated to three-phase four-wire grid during transition from grid outage to grid connected modes of operation
- Fig. 6.39 (a)-(b) Simulated performance of single-stage PV-BES system with bidirectional converter controlled BES integrated to three-phase four-wire grid at dynamic loading condition
- Fig. 6.40 (a)-(b) Simulated performance of single-stage PV-BES system with bidirectional converter controlled BES integrated to three-phase four-wire grid at variable solar insolation condition
- Fig. 6.41 (a)-(c) Harmonic spectra of load current (i_{La}), grid current (i_{La}) and load voltage (v_{La}) of of single-stage PV-BES system with bidirectional converter controlled BES integrated to three-phase four-wire grid
- Fig. 6.42 (a)-(b) Performance of single-stage PV-BES system integrated to three-phase grid with bidirectional converter controlled BES for MPPT at solar insolation level of (a) 1000 W/m^2 (b) 800 W/m^2
- Fig. 6.43 (a)-(d) Experimental performance of single-stage PV-BES system with bidirectional converter controlled BES integrated to three-phase four-wire grid during transition from grid connected to grid outage modes of operation
- Fig. 6.44 (a)-(d) Experimental performance of single-stage PV-BES system with bidirectional converter controlled BES integrated to three-phase four-wire grid during transition from grid outage to grid connected modes of operation
- Fig. 6.45 (a)-(b) Experimental Performance of single-stage PV-BES system with bidirectional converter controlled BES integrated to three-phase four-wire grid during transition at load unbalancing condition
- Fig. 6.46 (a)-(c) Experimental Performance of single-stage PV-BES system with bidirectional converter controlled BES integrated to three-phase four-wire grid during transition at variable solar insolation condition
- Fig. 6.47 (a)-(i) Experimental Performance of single-stage PV-BES system with bidirectional converter controlled BES integrated to three-phase four-wire grid at constant power feeding mode of operation
- Fig. 6.48 (a)-(d) Experimental performance of single-stage PV-BES system with bidirectional converter controlled BES integrated to three-phase four-wire grid during standalone mode of operation
- Fig. 7.1 Multiple PVs based DC charging of EVs interfaced with three-phase grid.
- Fig. 7.2 Multiple PVs based AC charging of EVs interfaced with three-phase grid.

- Fig. 7.3 Control Structure during grid connection of multiple PVs for DC charging of EVs
- Fig. 7.4 Control Structure during grid outage mode of multiple PVs for DC charging of EVs
- Fig. 7.5 EVs control algorithm during outage mode of operation
- Fig. 7.6 Control Structure of VSC1 for AC charging of EVs interfaced with multiple PVs
- Fig. 7.7 Control Structure of VSC2 for AC charging of EVs interfaced with multiple PVs
- Fig. 7.8 MATLAB model of multiple PVs interfaced with three-phase grid for DC charging of EVs
- Fig. 7.9 MATLAB model of multiple PVs interfaced with three-phase grid for AC charging of EVs
- Fig. 7.10 (a)-(c) Simulated performance of multiple PVs for DC charging of EVs during mode Transition between grid connected/ disconnected operation
- Fig. 7.11 (a)-(c) Harmonic Analysis of EVs DC charging interfaced with multiple PV arrays
- Fig. 7.12 (a)-(b) Simulated performance of multiple PVs for DC charging of EVs during load unbalancing condition
- Fig. 7.13 (a)-(b) Simulated performance of multiple PVs for DC charging of EVs during variable solar insolation condition
- Fig. 7.14 Real-time test bench with OPAL-RT controller for hardware in loop implementation of multiple PVs interfaced with three-phase grid for DC/ AC charging of electric vehicles
- Fig. 7.15 (a)-(c) Harmonic Analysis of grid-tied DC charging of EVs interfaced with multiple PV arrays
- Fig. 7.16 (a)-(b) Harmonic Analysis of standalone DC charging of EVs interfaced with multiple PV arrays
- Fig. 7.17 (a)-(g) Performance of multiple PVs interfaced with three-phase grid for DC charging of electric vehicles during mode transition from grid connected to disconnected modes of operation
- Fig. 7.18 (a)-(g) Performance of multiple PVs interfaced with three-phase grid for DC charging of electric vehicles during mode transition from grid disconnected to connected
- Fig. 7.19 (a)-(e) Performance of multiple PVs interfaced with three-phase grid for DC charging of electric vehicles during load unbalancing condition
- Fig. 7.20 (a)-(d) Performance of multiple PVs interfaced with three-phase grid for DC charging of electric vehicles during variable solar insolation condition
- Fig. 7.21 (a)-(b) Simulated performance of multiple PVs interfaced with three-phase grid for AC charging of electric vehicles during mode transition from grid connected to disconnected modes of operation
- Fig. 7.22 (a)-(c) Harmonic Analysis of grid interfaced AC charging of EVs interfaced with multiple PV arrays
- Fig. 7.23 (a)-(b) Simulated performance of multiple PVs interfaced with three-phase grid for AC charging of electric vehicles Mode transition from grid connected to disconnected modes of operation
- Fig. 7.24 (a)-(b) Simulated performance of multiple PVs interfaced with three-phase grid for AC charging of electric vehicles during load unbalancing condition
- Fig. 7.25 (a)-(b) Simulated performance of multiple PVs for AC charging of EVs during variable solar insolation condition
- Fig. 7.26 (a)-(e) Performance of multiple PVs interfaced with three-phase grid for AC charging of electric vehicles during mode transition from grid connected to disconnected modes of operation
- Fig. 7.27 (a)-(c) Harmonic Analysis of grid connected AC charging of EVs interfaced with multiple PV arrays

- Fig. 7.28 (a)-(b) Harmonic Analysis of grid connected AC charging of EVs interfaced with multiple PV arrays
- Fig. 7.29 (a)-(e) Performance of multiple PVs interfaced with three-phase grid for AC charging of electric vehicles during mode transition from grid disconnected to connected modes of operation
- Fig. 7.30 (a)-(g) Performance of multiple PVs interfaced with three-phase grid for AC charging of electric vehicles during load unbalancing condition
- Fig. 7.31 (a)-(e) Performance of multiple PVs interfaced with three-phase grid for AC charging of electric vehicles during variable solar insolation condition
- Fig. 8.1 Distributed microgrid consisting of solar, battery and fuel cell sources based common DC bus charging system for EVs
- Fig. 8.2 Distributed microgrid consisting of solar, wind, battery and fuel cell sources based common DC bus charging system for EVs
- Fig. 8.3 Control structure of common DC bus charging of EVs with grid-tied distributed microgrid consisting of solar, battery and fuel cell sources during grid connected mode of operation
- Fig. 8.4 Control structure of common DC bus charging of EVs during standalone mode of operation with distributed microgrid consisting of solar, battery and fuel cell sources
- Fig. 8.5 Control structure of common DC bus charging of EVs during grid-tied and standalone modes of operation with distributed microgrid consisting of solar, wind, battery and fuel cell sources
- Fig. 8.6 MATLAB model of distributed microgrid consisting of solar, battery and fuel cell sources for DC charging of EVs
- Fig. 8.7 MATLAB model of distributed microgrid consisting of solar, wind, battery and fuel cell sources for DC charging of EVs
- Fig. 8.8 (a)-(b) Simulated performance of common DC bus EVs charging with distributed microgrid consisting of solar, battery and fuel cell sources during mode change between grid connection to disconnection modes of operation
- Fig. 8.9 (a)-(b) Simulated performance of common DC bus EVs charging with distributed microgrid consisting of solar, battery and fuel cell sources during mode change between grid disconnection to connection modes of operation
- Fig. 8.10 (a)-(d) Simulated performance of common DC bus EVs charging with distributed microgrid consisting of solar, battery and fuel cell sources for EV power variation during grid connection/disconnection modes of operation
- Fig. 8.11 (a)-(b) Performance of common DC bus EVs charging with distributed microgrid consisting of solar, battery and fuel cell sources during load unbalancing condition
- Fig. 8.12 (a)-(b) Performance of common DC bus EVs charging with distributed microgrid consisting of solar, battery and fuel cell sources during variable solar insolation condition
- Fig. 8.13 (a)-(c) Harmonic analysis of grid current, load current and load voltage with distributed microgrid consisting of solar, battery and fuel cell sources for common DC bus charging of EVs
- Fig. 8.14 (a)-(g) Performance of common DC bus EVs charging with distributed microgrid consisting of solar, battery and fuel cell sources during mode change between grid connection to disconnection modes of operation
- Fig. 8.15 (a)-(h) Performance of common DC bus EVs charging with distributed microgrid consisting of solar, battery and fuel cell sources during mode change between grid disconnection to connection modes of operation

- Fig. 8.16 (a)-(d) Performance of common DC bus EVs charging with distributed microgrid consisting of solar, battery and fuel cell sources for EV power variation during grid connection/disconnection modes of operation
- Fig. 8.17 (a)-(c) Harmonic Analysis of grid-tied DC charging of EVs with distributed microgrid consisting of solar, battery and fuel cell sources
- Fig. 8.18 (a)-(b) Harmonic Analysis of standalone DC charging of EVs with distributed microgrid consisting of solar, battery and fuel cell sources
- Fig. 8.19 (a)-(e) Performance of common DC bus EVs charging with distributed microgrid consisting of solar, battery and fuel cell sources during variable solar insolation condition
- Fig. 8.20 (a)-(e) Performance of common DC bus EVs charging with distributed microgrid consisting of solar, battery and fuel cell sources during load unbalancing condition
- Fig. 8.21 (a)-(d) Performance of common DC bus EVs charging with distributed microgrid consisting of solar, battery and fuel cell sources during constant grid power feeding mode of operation
- Fig. 8.22 (a)-(b) Simulated performance of common DC bus EVs charging with distributed microgrid consisting of solar, wind, battery and fuel cell sources during mode change between grid connection to disconnection
- Fig. 8.23 (a)-(c) Harmonic Analysis of grid current, load current and load voltage for common DC bus charging of EVs with distributed microgrid consisting of solar, wind, battery and fuel cell sources
- Fig. 8.24 (a)-(b) Simulated performance of common DC bus EVs charging with distributed microgrid consisting of solar, wind, battery and fuel cell sources during mode change between grid disconnection to connection
- Fig. 8.25 (a)-(b) Simulated performance of common DC bus EVs charging with distributed microgrid consisting of solar, wind, battery and fuel cell sources during load unbalancing condition
- Fig. 8.26 (a)-(b) Simulated performance of common DC bus EVs charging with distributed microgrid consisting of solar, wind, battery and fuel cell sources during constant grid power feeding with wind speed variation condition
- Fig. 8.27 (a)-(b) Simulated performance of common DC bus EVs charging with distributed microgrid consisting of solar, wind, battery and fuel cell sources during variable solar insolation condition
- Fig. 8.28 (a)-(h) Performance of common DC bus EVs charging with distributed microgrid consisting of solar, wind, battery and fuel cell sources during mode change between grid connection to disconnection
- Fig. 8.29 (a)-(c) Harmonic Analysis of grid current, load current and load voltage during grid tied mode for common DC bus charging of EVs with distributed microgrid consisting of solar, wind, battery and fuel cell sources
- Fig. 8.30 (a)-(b) Harmonic Analysis of load current and load voltage during standalone mode for common DC bus charging of EVs with distributed microgrid consisting of solar, wind, battery and fuel cell sources
- Fig. 8.31 (a)-(h) Performance of common DC bus EVs charging with distributed microgrid consisting of solar, wind, battery and fuel cell sources during mode change between grid disconnection to connection modes of operation
- Fig. 8.32 (a)-(e) Performance of common DC bus EVs charging with distributed microgrid consisting of solar, wind, battery and fuel cell sources during load unbalancing condition

- Fig. 8.33 (a)-(e) Performance of common DC bus EVs charging with distributed microgrid consisting of solar, wind, battery and fuel cell sources during variable solar insolation condition
- Fig. 8.34 (a)-(e) Performance of common DC bus EVs charging with distributed microgrid consisting of solar, wind, battery and fuel cell sources during constant power feeding wind speed variation condition
- Fig. 9.1 Distributed microgrids consisting of solar, battery and fuel cell sources based common AC bus charging system for EVs
- Fig. 9.2 Distributed microgrids consisting of solar, wind, battery and fuel cell sources based common AC bus charging system for EVs
- Fig. 9.3 Control Structure of VSC1 for common AC bus charging of EVs consisting of solar PV array interfaced with three-phase grid
- Fig. 9.4 Control structure of VSC2 for common AC bus charging of EVs consisting of fuel cell stack interfaced with three-phase grid
- Fig. 9.5 Control structure of VSC3 for common AC bus charging of EVs consisting of PMSG driven wind turbine interfaced with three-phase grid
- Fig. 9.6 MATLAB model of distributed microgrids consisting of solar and fuel cell sources for AC charging of EVs
- Fig. 9.7 MATLAB model of distributed microgrids consisting of solar, wind and fuel cell sources for AC charging of EVs
- Fig. 9.8 (a)-(b) Simulated performance of common AC bus EVs charging with distributed microgrids consisting of solar, battery and fuel cell sources during mode change between grid connection to disconnection modes of operation
- Fig. 9.9 (a)-(b) Simulated performance of common AC bus EVs charging with distributed microgrids consisting of solar, battery and fuel cell sources during mode change between grid disconnection to connection modes of operation
- Fig. 9.10 (a)-(b) Simulated performance of common AC bus EVs charging with distributed microgrids consisting of solar, battery and fuel cell sources during variable solar insolation condition
- Fig. 9.11 (a)-(b) Simulated performance of common AC bus EVs charging with distributed microgrids consisting of solar, battery and fuel cell sources during load unbalancing condition
- Fig. 9.12 (a)-(b) Simulated performance of common AC bus EVs charging with distributed microgrids consisting of solar, battery and fuel cell sources during constant grid power feeding mode of operation
- Fig. 9.13 (a)-(c) Harmonic Analysis with distributed microgrids consisting of solar, battery and fuel cell sources for common AC bus charging of EVs
- Fig. 9.14 (a)-(e) Performance of common AC bus EVs charging with distributed microgrids consisting of solar, battery and fuel cell sources during mode change between grid connection to disconnection modes of operation
- Fig. 9.15 (a)-(e) Mode change between grid disconnection to connection for common AC bus EVs charging with distributed microgrids consisting of solar, battery and fuel cell sources
- Fig. 9.16 (a)-(d) Performance of common AC bus EVs charging with distributed microgrids consisting of solar, battery and fuel cell sources during load unbalancing condition
- Fig. 9.17 (a)-(d) Performance of common AC bus EVs charging with distributed microgrids consisting of solar, battery and fuel cell sources during variable solar insolation condition

- Fig. 9.18 (a)-(e) Harmonic Analysis during grid interconnection and disconnection with distributed microgrids consisting of solar, battery and fuel cell sources for common AC bus charging of EVs
- Fig. 9.19 (a)-(d) Performance of common AC bus EVs charging with distributed microgrids consisting of solar, battery and fuel cell sources during constant grid power feeding mode of operation
- Fig. 9.20 (a)-(b) Simulated performance of common AC bus EVs charging with distributed microgrids consisting of solar, wind, battery and fuel cell sources during mode change between grid connection to disconnection modes of operation
- Fig. 9.21 (a)-(c) Harmonic Analysis with distributed microgrids consisting of solar, wind, battery and fuel cell sources for common AC bus charging of EVs
- Fig. 9.22 (a)-(b) Simulated performance of common AC bus EVs charging with distributed microgrids consisting of solar, wind and fuel cell sources during mode change between grid disconnection to connection modes of operation
- Fig. 9.23 (a)-(b) Simulated performance of common AC bus EVs charging with distributed microgrids consisting of solar, wind and fuel cell sources during variable solar insolation condition
- Fig. 9.24 (a)-(b) Simulated performance of common AC bus EVs charging with distributed microgrids consisting of solar, wind and fuel cell sources during load removal condition
- Fig. 9.25 (a)-(b) Simulated performance of common AC bus EVs charging with distributed microgrids consisting of solar, wind and fuel cell sources for Constant grid power feeding mode during wind speed variation condition
- Fig. 9.26 (a)-(f) Performance of common AC bus EVs charging with distributed microgrids consisting of solar, wind and fuel cell sources during mode change between grid connection to disconnection modes of operation
- Fig. 9.27 (a)-(c) Harmonic Analysis during grid interconnection with distributed microgrids consisting of solar, wind and fuel cell sources for common AC bus charging of EVs
- Fig. 9.28 (a)-(b) Harmonic Analysis during islanded mode of operation with distributed microgrids consisting of solar, wind and fuel cell sources for common AC bus charging of EVs
- Fig. 9.29 (a)-(f) Performance of common AC bus EVs charging with distributed microgrids consisting of solar, wind and fuel cell sources during mode change between grid disconnection to connection modes of operation
- Fig. 9.30 (a)-(d) Performance of common AC bus EVs charging with distributed microgrids consisting of solar, wind, battery and fuel cell sources during load removal condition
- Fig. 9.31 (a)-(d) Performance of common AC bus EVs charging with distributed microgrids consisting of solar, wind, battery and fuel cell sources during variable solar insolation condition
- Fig. 9.32 (a)-(d) Performance of common AC bus EVs charging with distributed microgrids consisting of solar, wind, battery and fuel cell sources during wind speed variation condition

LIST OF TABLES

Table 3.1	Design Parameters of Three-Phase Grid Interactive Single-Stage PV System for Experimental Implementation
Table 3.2	Design Parameters of Double-Stage PV System Interfaced to the Grid for Experimental Implementation
Table 4.1	Design Parameters of Three-Phase Four-Wire Grid Interactive Single-Stage PV System for Experimental Implementation
Table 4.2	Design Parameters of Double-Stage PV System Interfaced to the Three-Phase Four-Wire Grid for Experimental Implementation
Table 5.1	Design Parameters of Double-Stage PV-BES System Integrated to Three-Phase Grid for Experimental Implementation
Table 5.2	Design Parameters of Double-Stage PV-BES System Integrated to Three-Phase Grid with Bidirectional Converter Controlled BES for Experimental Implementation
Table 5.3	Design Parameters of Single-Stage PV-BES System Integrated to Three-Phase Grid with Bidirectional Converter Controlled BES for Experimental Implementation
Table 6.1	Design Parameters of Double-Stage PV-BES System Integrated to Three-Phase Four-Wire Grid for Experimental Implementation
Table 6.2	Design Parameters of Double-Stage PV-BES System Integrated to Three-Phase Four-Wire Grid with Bidirectional Converter Controlled BES for Experimental Implementation
Table 6.3	Design Parameters of Single-Stage PV-BES System Integrated to Three-Phase Four-Wire Grid with Bidirectional Converter Controlled BES for Experimental Implementation
Table 7.1	Design Parameters of Three-Phase Grid Connected Multiple PV arrays for DC Charging of EVs
Table 7.2	2 Design Parameters of Three-Phase Grid Connected Multiple PV arrays for AC Charging of EVs
Table 8.1	Design Parameters of Distributed Microgrid Consisting of Solar, Battery and Fuel Cell Sources for DC Charging of EVs
Table 8.2	Design Parameters of Distributed Microgrid Consisting of Solar, Battery, Wind and Fuel Cell Sources for DC Charging of EVs
Table 9.1	Design Parameters of Distributed Microgrids Consisting of Solar, Battery and Fuel Cell Sources for Common AC Bus Charging of EVs
Table 9.2	2 Design Parameters of Distributed Microgrids Consisting of Solar, Wind, Battery and Fuel Cell Sources for Common AC Bus Charging of EVs

LIST OF ABBREVIATIONS

DERs	Distributed Energy Sources
PV	Photovoltaic
EV	Electric Vehicles
FC	Fuel Cells
WT	Wind Turbines
DG	Distributed Generation
STSs	Static Transfer Switches
PLLs	Phase Locked Loops
LMF	Least Mean Fourth
LMS	Lean Mean Square
GI	Generalized Integrators
PCC	Point Of Common Coupling
MPP	Maximum Power Point
P&O	Perturb And Observe
FCVs	Fuel Cell Vehicles
EVCS	EV Charging Systems
DC	Direct Current
AC	Alternating Current
RESs	Renewable Energy Sources
PQ	Power Quality
VSC	Voltage Source Converter
INC	Incremental Conductance
UPF	Unity Power Factor
S&H	Sample/Hold Logic
ZCD	Zero Crossing Detector
PR	Proportional Resonant
ADCs	Analog To Digital Converters
FPGA	Field Programmable Gate Array
DIO	Digital Inputs And Outputs
DSO	Digital Storage Oscilloscope
CLBs	Configurable Logic Blocks
ADC	Analog To Digital Conversion
THD	Total Harmonic Distortion
IGBTs	Insulated Gate Bipolar Transistors
LTI-EPLL	Linear Time Invariant Enhanced Phase Locked Loop
VDFs	Variable Digital Filters
PI	Proportional Integral
BES	Battery Energy Storage
SOC	State Of Charge
PEM	Proton Exchange Membrane
PMSG	Permanent Magnet Synchronous Generator
WGC	Wind Power Generating Converter

LIST OF SYMBOLS

i_{La}, i_{Lb}, i_{Lc}	Load currents
I_{pv}	PV current
i_{sa}, i_{sb}, i_{sc}	Grid currents
v_{sab}, v_{sbc}	Grid line voltages
v_{sa}, v_{sb}, v_{sc}	Grid phase voltages
$i_{VSCa}, i_{VSCb}, i_{VSCc}$	VSC currents
V_{dc}	DC link voltage
C_f, R_f	Ripple filter
V_{pv}	PV voltage
L_b	Boost inductor
S_b	Switching pulses of Boost inductor
$i_{Lfa}, i_{Lfb}, i_{Lfc}$	Fundamental of load currents
u_{qa}, u_{qb}, u_{qc}	Quadrature-phase unit templates
u_{pa}, u_{pb}, u_{pc}	In-phase unit templates
V_{dc}^*	Reference DC link voltage
$h_0, \alpha_1, h_1, \alpha_2, k_1$	Gains of Adaptive Digital Filter
$I_{fpa}, I_{fpb}, I_{fpc}$	Load active power components
I_{loss}	DC loss component
I_{pLavg}	Load active power
I_{pnet}	Grid active power
V_{dce}	Voltage error
$i_{sa}^*, i_{sb}^*, i_{sc}^*$	Reference Grid currents
V_t	Terminal voltage
P_{pv}	Solar PV power
θ_g, θ_L	Grid voltage angle and load voltage angle
$i_{La}^*, i_{Lb}^*, i_{Lc}^*$	Reference Load currents
$v_{La}^*, v_{Lb}^*, v_{Lc}^*$	Reference Load voltages
ω_L	Load frequency
ω_e	Frequency error
θ_e	Phase error
θ_m	Modified load voltage angle
$\sigma_1, \gamma_1, \beta$	Gains of Subband Adaptive Filter
w_{pv}	PV Feed-forward term
f_g	Grid frequency
V_{ref}	Amplitude of load voltage
$T_a(s), T_b(s), T_c(s)$	Transfer function of PR controllers
$G_{insolation}$	Solar insolation level
C_{dc}	DC link capacitance
i_{sn}, i_{Ln}, i_{VSCn}	Neutral currents of grid, load and VSC
L_n	Neutral leg interfacing inductor
L_f	Interfacing inductor
μ, k_1, k_2, k_3	Gains of adaptive transversal filter with leaky integrator
k_1, k_2	Gains of recursive transversal filter
ω_{ca}	cut-off frequency
f_{center}	Centre frequency
$V_{batt}, I_{batt}, P_{batt}$	Battery voltage, battery current and battery power
L_{bb}	Bidirectional buck-boost converter

σ_1, σ_2, k	Gains of digital decimation filter
w_{batt}	Battery feed-forward term
β_1, β_2	Gains of variable fractional delay filter
I_{batt}^*	Reference battery current
I_{battr}	Battery current error
γ_1, γ_2	Gains of fractional Lagrange filter
$D(m)$	Duty cycle of bidirectional converter
a, γ	Gains of combined IIR and FIR filter
k, β_1, β_2	Gains of suboptimal filter
I_{ev}, P_{ev}, V_{ev}	EVs current, power and voltage
$I_{pv1}, P_{pv1}, V_{pv1}$	PV ₁ array current, power and voltage
$I_{pv2}, P_{pv2}, V_{pv2}$	PV ₂ array current, power and voltage
$i_{VSCa1}, i_{VSCb1}, i_{VSCc1}$	VSC currents of unit ₁
$i_{VSCa2}, i_{VSCb2}, i_{VSCc2}$	VSC currents of unit ₂
$i_{La1}, i_{Lb1}, i_{Lc1}$	Load currents of unit ₁
$i_{La2}, i_{Lb2}, i_{Lc2}$	Load currents of unit ₂
k_1, k_2, k_3	Gains of variable digital filter
I_{fc}, P_{fc}, V_{fc}	Fuel cell current, power and voltage
E_n	Nerst voltage of fuel cell
$i_{gena}, i_{genb}, i_{genc}$	PMSG stator generator currents
T_e	Electromagnetic torque
$h_0, h_1, \alpha_1, \alpha_2$	Gains of warped digital filter
$i_{VSCa3}, i_{VSCb3}, i_{VSCc3}$	VSC currents of unit ₃
$i_{La3}, i_{Lb3}, i_{Lc3}$	Load currents of unit ₃
γ	Gain of Biquad filter